Biology Open (2015) 4, 1595-1607 doi:10.1242/bio.013151

et al. (2011) have reported that the long-term self-renewal of hESC-derived neural stem cells is sustained by a chemically defined medium supplemented with LIF, CHIR99021 and SB431542 (TGF-β inhibitor). Thus, these findings suggest that the GSK3β and TGF-β pathways are not essential for the self-renewal of LIF-dependent primitive NSCs. This evidence is in line with our data, which showed that the colonies of LD-iNSCs also grow in medium supplemented with LIF, CHIR99021 and SB431542 (Fig. S4B). In our study, LD-iNSCs colonies were formed in the presence of PD0325901 (inhibitor of ERK1/2 phosphorylation) instead of SB431542. This observation suggested that 2i/LIF promotes the conversion of human fibroblasts to primitive NSCs when accompanied by ectopic expression of reprogramming factors, but does not elicit a self-renewal response in hiPSCs. Gafni et al. (2013) recently showed that naïve pluripotent stem cells can be established in humans using a unique combination of cytokines and small molecule inhibitors in addition to 2i/LIF; this medium, termed naïve human stem cell medium (NHSM; Fig. 8B), further supported the concept that culture environments could control the fate of reprogrammed cells (Han et al., 2011). As described above, LD-iNSCs may metastably settle into a state poised toward pluripotency, suggesting that the replacement of 2i/LIF with NHSM may elevate LD-iNSCs to a more pluripotent status from the standpoint of the hierarchy of pluripotency.

In summary, we successfully developed methods for the direct generation of LIF-dependent primitive iNSCs from human fibroblasts in the presence of 2i/LIF. Our methods may be applied to cells isolated from patients with neurological disorders, such as Parkinson's disease, amyotrophic lateral sclerosis, Alzheimer's disease, or other neurodegenerative diseases. These patient-specific LD-iNSCs should be useful in future drug screening and for the modeling certain neurological diseases.

LD-iNSCs can be stably expanded for more than 100 passages in the presence of 2i/LIF/Dox, suggesting that the plasticity of the LD-iNSCs is maintained in the long run. In the future, LD-iNSCs may also turn out to be useful for cell therapy, for e.g. patients with spinal cord injury. In conclusion, this study might open the possibility of generating LD-iNSCs from patients for cell therapy and for identification of drug targets in neurological diseases.

MATERIALS AND METHODS

Ethics statement

Primary human fibroblasts were used with approval from the Institutional Review Board of the National Institute for Child Health and Development, Japan. Signed informed consent forms were obtained from the donors, and the surgical specimens were irreversibly de-identified. All experiments that involved handling of human cells and tissues were performed in line with the tenets of the Declaration of Helsinki.

Animal experiments

Research involving animals complied with the protocols approved by the Institutional Animal Care and Use Committee of the National Research Institute for Child Health and Development.

Generation of LD-iNSCs

LD-iNSCs were produced using the following procedure. BJ foreskin fibroblasts were purchased from American Type Culture Collection (ATCC) – alternatively, primary human fibroblast-like cells from menstrual blood were isolated as described previously (Cui et al., 2007) – and grown in 10% fetal bovine serum (FBS)/Dulbecco's modified Eagle medium (DMEM); the cells displayed a spindle-shaped morphology. Primary human fibroblasts (1.5×10^5) were plated in a 6-well plate; after 24 h, two lentiviral vectors (carrying doxycycline-inducible TRE3G promoter-driven human *OCT4*, *KLF4*, *SOX2*, *L-MYC* and *NANOG* and the CAG promoter-driven Tet-On 3G transactivator) were transduced into the cells. Three days after the transduction, primary human fibroblasts were passaged by trypsinization, and re-plated on irradiated mouse embryonic fibroblast (MEF) feeder layers. LD-iNSCs were induced by replacing the medium with LD-iNSC induction medium supplemented with 0.5× Knockout DMEM/F12 medium (Life Technologies, Carlsbad, CA, USA), 0.5× Knockout Neurobasal Medium (Life Technologies), 0.5× B27 (Life Technologies), 0.5× N2 supplement (Life Technologies), 10 μg/ml recombinant human insulin (Wako Pure Chemical Industries, Osaka, Japan), 0.1% recombinant human LIF (Wako Pure Chemical Industries), 0.005% bovine albumin fraction V (Life Technologies), 1% GlutaMAX (Life Technologies), 1% nonessential amino acids (Life Technologies), 55 nM β-mercaptoethanol (Life Technologies), 100 U/ml penicillin-streptomycin (Life Technologies), 2% KnockOut Serum Replacement (Life Technologies), and 64 μg/ml L-ascorbic acid-2-phosphate magnesium (Sigma-Aldrich, St. Louis, MO, USA). Neural progenitor-like round-shaped colonies usually appeared after 14–28 days. The colonies were picked, seeded in individual wells, and cultured on MEF feeder layers with the LD-iNSC induction medium supplemented with two small molecule inhibitors (2i): PD0325901 (1 μM, ERK1/2 inhibitor; Wako Pure Chemical Industries) and CHIR99021 (3 μM, GSK3β inhibitor; Axon Medchem, Fairfax, VA, USA). The cells were seeded at $>2\times10^5$ cells per 60-mm dish using Accutase (Life Technologies) every 3–4 days, depending on the culture density. LD-iNSCs and hiPSCs cells were collected using Accutase, and resuspended in buffer R (provided with the *Neon* Electroporation System; Life Technologies) for transfection; the resuspended cells were transfected with 3 μg of the DNA constructs using the Neon Transfection System (Life Technologies; 1400 V, 10 ms, 3 pulses for LD-iNSCs; 1050 V, 30 ms, 2 pulses for hiPSCs).

Although the LD-iNSCs established in this study were successfully maintained as described above, LD-iNSCs could also be grown in Geltrex-coated plates for at least one month. Moreover, according to the conventional culture conditions for primitive NSCs, LD-iNSC induction medium supplemented with 3 μM CHIR99021 and 2 μM SB431542 (TGF-β inhibitor; Tocris Bioscience, Bristol, UK) under feeder-free (Matrigel) culture conditions (Li et al., 2011) was also used.

Derivation of hiPSCs

LD-iNSCs were plated at a density of 1.5×10^5 cells per 100-mm dish on MEF feeder layers in LD-iNSC induction medium, in the presence of 2i/LIF/Dox. Dox was removed from the medium the next day, and the cells were further maintained in hESC medium containing Knockout DMEM supplemented with 20% Knockout serum replacement, 10 ng/ml recombinant human bFGF (Life Technologies), 1% GlutaMAX, 1% nonessential amino acids, 55 nM β-mercaptoethanol, 1 mM sodium pyruvate (Life Technologies), and 100 U/ml penicillin-streptomycin. Typical hiPSC-like colonies emerged after approximately 3 weeks, and were mechanically picked and seeded on fresh MEF feeder layers. The colonies were passaged mechanically every 5–7 days.

Neural differentiation *in vitro*

As shown in Figs 4A and 5A, the protocol for *in vitro* differentiation of LD-iNSCs into motor neurons or dopaminergic neurons was modified from a previously reported method (Li et al., 2011). The development of motor neurons can be recapitulated *in vitro* by the addition of RA and an SHH agonist (Hh-Ag1.3) to the culture medium of ESCs (Wichterle et al., 2002). Based on this evidence, we used the procedure shown in Fig. 4A to differentiate LD-iNSCs into motor neurons. LD-iNSCs were plated on dishes coated with laminin/poly-L-ornithine, and treated with 0.1 mM RA and SHH (100 ng/ml) for 7 days. These cells were then cultured in the presence of 0.1 mM RA and the SHH (50 ng/ml) for 7 days, and finally cultured in the differentiation medium supplemented with 10 ng/ml brain-derived neurotrophic factor (BDNF) and 10 ng/ml glial cell-derived neurotrophic factor (GDNF). The protocol shown in Fig. 5A was used for DA neuron differentiation. In this protocol, LD-iNSCs or hESC (H9)-derived NSCs (Life Technologies) were first treated with 10 ng/ml BDNF and 10 ng/ml GDNF for two weeks, and subsequently with 100 ng/ml SHH and 100 ng/ml FGF8b for 10 days.

Biology Open (2015) 4, 1595-1607 doi:10.1242/bio.013151

Finally, these cells were further differentiated in the presence of 10 ng/ml BDNF, 10 ng/ml GDNF, 10 ng/ml insulin-like growth factor (IGF)-1, 1.0 ng/ml TGF-β3, and 0.5 mM dibutyryl-cAMP (dbcAMP) for another 2–3 weeks.

RNA expression analysis

RNA was isolated from sub-confluent growing cells using the RNeasy Mini Kit (Qiagen, Venlo, Netherlands), and DNA was removed using DNase (Life Technologies) to avoid genomic DNA amplification. First-strand cDNA was synthesized from 2 μg RNA using SuperScript III reverse transcriptase and an oligo-dT primer (Life Technologies) according to the manufacturer protocols. PCR reactions were performed using TaKaRa Ex Taq Hot Start (Takara Bio Inc., Shiga, Japan). The PCR primer sequences are summarized in Table S2. All PCR products were analyzed by 2% agarose gel electrophoresis, staining with ethidium bromide, and visualizing the stained gels under ultraviolet light. Quantitative PCR (q-PCR) was performed in triplicate on a QuantStudio 12K Flex Real-Time PCR System (Applied Biosystems, Waltham, MA, USA) using the SYBR Green PCR Master mix (Applied Biosystems). Dissociation curves were constructed after amplification to ensure the amplification of each PCR product. All primer sequences are summarized in Table S2. QuantStudio 12K Flex Software v1.0 was used to quantify the expression of each mRNA segment. Glyceraldehyde 3-phosphate dehydrogenase (*GAPDH*), a housekeeping control gene, was used for normalization.

Alkaline phosphatase staining and immunofluorescence analysis

Alkaline phosphatase activity was determined using the BCIP/NBT Substrate System (Dako, Glostrup, Denmark). For immunofluorescent staining, the cells were fixed with 4% paraformaldehyde in phosphate-buffered saline (PBS; Wako Pure Chemical Industries) for 5 min at 4°C, and permeabilized with 0.2% Triton X-100 for 2 min at room temperature. The fixed cells were blocked with a normal serum solution (Dako) at room temperature. The following primary antibodies were used: mouse anti-Oct4 (Santa Cruz Biotechnology, Santa Cruz, CA, USA), mouse anti-Nanog (ReproCELL, Yokohama, Japan), rabbit anti-Sox2 (Merck-Millipore, Darmstadt, Germany), mouse anti-SSEA4 (Millipore), mouse anti-TRA-1-81 (Millipore), rabbit anti-Sox1 (Abcam, Cambridge, UK), rabbit anti-Pax6 (Abcam), rabbit anti-Nestin (Sigma-Aldrich), rabbit anti-BLBP (Millipore), mouse anti-Ki-67 (BD Pharmingen, Franklin Lakes, NJ), mouse anti-βIII tubulin (Promega Corp., Madison, WI, USA), rabbit anti-GFAP (Sigma-Aldrich), mouse anti-O4 (Merck-Millipore), rabbit anti-GFAP (DAKO), rabbit anti-HB9 (Abcam), rabbit anti-Islet1 (Abcam), rabbit anti-HoxC8 (Abcam), goat anti-ChAT (Merck-Millipore), rabbit anti-EN-1 (Santa Cruz Biotechnology), rabbit anti-FoxA2 (Merck-Millipore), rabbit anti-Lmx1 (Merck-Millipore), rabbit anti-Nurr1 (Santa Cruz Biotechnology), and rabbit anti-tyrosine hydroxylase (Merck-Millipore). The day after incubation at 4°C with a primary antibody, the cells were incubated with the appropriate secondary antibody (Life Technologies) for 60 min at room temperature. The cell nuclei were counterstained with DAPI (0.5 mg/ml). The staining was visualized using a laser scanning confocal microscope (Carl Zeiss).

Teratoma formation assay

hiPSCs were suspended at 1×10^7/ml in PBS. The cell suspension (100 μl, 10^6 cells) was injected subcutaneously into the dorsal flank of nude mice (Clea Japan, Tokyo, Japan). Two to three months after the injection, the tumors were surgically excised from the mice. The tumor specimens were fixed in PBS containing 4% formaldehyde, and embedded in paraffin. The sections were histologically examined after hematoxylin and eosin staining.

ChIP q-PCR

Feeder-free iPS cells (2×10^7) were harvested by trypsinization and fixed in formaldehyde (final concentration 1%). The formaldehyde-fixed cells (5×10^6) were resuspended in NP-40 lysis buffer (ChIP Reagent; Nippon Gene Co., Ltd., Tokyo, Japan) containing a 1× protease inhibitor mix (P.I.; Nippon Gene Co., Ltd.), mixed well by vortexing, and incubated on ice for 10 min. The cells were then resuspended in sodium dodecyl sulfate (SDS) lysis buffer (ChIP Reagent; Nippon Gene Co., Ltd.) and the lysate was sonicated to fragment chromatin using a Covaris S220 focused-ultrasonicator. The chromatin was purified by centrifugation and immunoprecipitated with protein A-beads (Veritas Prep., Malibu, CA, USA) conjugated to an anti-H3K4me3 antibody (Millipore) or rabbit IgG (Abcam) in Buffer A with P.I. (LowCell ChIP kit; Diagenode, Liege, Belgium) overnight at 4°C. The chromatin-containing beads were washed with Buffers A and C (LowCell ChIP kit). The washed chromatin-containing beads were incubated in ChIP direct elution buffer (ChIP Reagent) for 20 min at 95°C, and then incubated with proteinase K for 2 h at 55°C. DNA immunoprecipitated from the supernatant was purified using Agencourt AMPure XP beads (Beckman Coulter, Pasadena, CA, USA) according to the manufacturer protocols. The samples were subjected to q-PCR using SYBR Green (Life Technologies). The primer sequences are summarized in Table S2.

Bisulfite sequencing

Genomic DNA was isolated from 10^2–10^7 cells using the NucleoSpin Tissue Kit (Macherey-Nagel, Duren, Germany) and 200–500 ng of the isolated DNA was further treated with bisulfite (EZ DNA Methylation-Gold Kit; Zymo Research, Irvine, CA, USA), according to instructions provided by the manufacturers. The bisulfite treatment converted all unmethylated cytosine bases to uracil, while methylated cytosine remained unchanged. The promoter regions of *OCT4*, *REX1* and *NANOG* were amplified by PCR for bisulfite DNA sequencing, using primers listed in Table S2. PCR conditions were as follows: 35–40 cycles of denaturation at 94°C for 30 s, annealing at 58°C for 30 s, and extension at 72°C for 60 s, using the KAPA HiFi HotStart Uracil+ kit (Kapa Biosystems, Wilmington, MA, USA). The amplified DNA product (with the correct size) was isolated by 2% agarose gel electrophoresis, purified using a QIAquick Gel Extraction kit (Qiagen), and ligated into the pGEM-T easy vector (Promega Corp.). More than 10 clones were randomly picked per cell sample for sequencing. A detailed profile of the DNA methylation sites was analyzed using QUMA (Kumaki et al., 2008).

DNA/RNA *fluorescence in situ* hybridization (FISH)

Cells were harvested using Accutase (Life Technologies); a single-cell suspension was prepared and plated on vitronectin-coated chamber slides. The cells grown on chamber slides were treated with 0.005% pepsin/0.1 N HCl for 3 min, and fixed in 4% paraformaldehyde for 30 min. cDNA probes specific to the XIST exon 1 and 6 regions were generated for XIST detection; these were labeled by nick translation using the Cy3-labeled dUTP. The HXO-10 probe (Chromosome Science Labo Inc., Sapporo, Japan) was used for the detection of X chromosome. The reaction mixtures containing the XIST DNA and HXO-10 probes were combined for RNA FISH, and added to the cells on the slide. The probes were carefully covered with a coverslip and incubated overnight. The slides were subsequently washed, and a DAPI mounting medium was applied to each cell spot. FISH signals were visualized using a Leica DMRA2 microscope (Leica, Wetzlar, Germany). Images were acquired using CW4000-FISH (Leica). All FISH analyses were performed commercially by Chromosome Science Labo Inc.

Acknowledgements

We would like to thank Drs Kevin Eggan (Harvard University) and Justin Ichida (University of Southern California) for the helpful discussions and Masakazu Machida (National Center for Child Health and Development) for their valuable technical assistance.

Competing interests

The authors declare no competing or financial interests.

Author contributions

T.M. and H.A. designed the study. T.M., T.S., A.F., R.T. and T.K. performed the experiments. T.M., T.S., A.F., R.T., T.K. and H.A. analyzed the data. A.U. and H.A. supervised the study. T.M. and H.A. wrote the manuscript.

Funding
This research was supported in part by a Grant-in-Aid for Scientific Research (B) [JSPS 26293364], for challenging Exploratory Research [JSPS 25670710] to H.A. and for Young Scientists (B) ([JSPS 21791580] to T.M.; a grant from the Japanese Ministry of Health, Labor and Welfare to H.A. and A.U.; and a grant from Core Research for Evolutional Science and Technology (JST-CREST) to H.A. H.A. is also supported by grants from the National Center for Child Health and Development [26-1 and 24-6].

Supplementary information
Supplementary information available online at
http://bio.biologists.org/lookup/suppl/doi:10.1242/bio.013151/-/DC1

References

Akamatsu, W., DeVeale, B., Okano, H., Cooney, A. J. and van der Kooy, D. (2009). Suppression of Oct4 by germ cell nuclear factor restricts pluripotency and promotes neural stem cell development in the early neural lineage. *J. Neurosci.* **29**, 2113-2124.

Bernstein, B. E., Mikkelsen, T. S., Xie, X., Kamal, M., Huebert, D. J., Cuff, J., Fry, B., Meissner, A., Wernig, M., Plath, K. et al. (2006). A bivalent chromatin structure marks key developmental genes in embryonic stem cells. *Cell* **125**, 315-326.

Bodnar, A. G., Ouellette, M., Frolkis, M., Holt, S. E., Chiu, C.-P., Morin, G. B., Harley, C. B., Shay, J. W., Lichtsteiner, S. and Wright, W. E. (1998). Extension of life-span by introduction of telomerase into normal human cells. *Science* **279**, 349-352.

Buecker, C., Chen, H.-H., Polo, J. M., Daheron, L., Bu, L., Barakat, T. S., Okwieka, P., Porter, A., Gribnau, J., Hochedlinger, K. et al. (2010). A murine ESC-like state facilitates transgenesis and homologous recombination in human pluripotent stem cells. *Cell Stem Cell* **6**, 535-546.

Caiazzo, M., Dell'Anno, M. T., Dvoretskova, E., Lazarevic, D., Taverna, S., Leo, D., Sotnikova, T. D., Menegon, A., Roncaglia, P., Colciago, G. et al. (2011). Direct generation of functional dopaminergic neurons from mouse and human fibroblasts. *Nature* **476**, 224-227.

Cao, F., Xie, X., Gollan, T., Zhao, L., Narsinh, K., Lee, R. J. and Wu, J. C. (2010). Comparison of gene-transfer efficiency in human embryonic stem cells. *Mol. Imaging Biol.* **12**, 15-24.

Clouaire, T., Webb, S., Skene, P., Illingworth, R., Kerr, A., Andrews, R., Lee, J.-H., Skalnik, D. and Bird, A. (2012). Cfp1 integrates both CpG content and gene activity for accurate H3K4me3 deposition in embryonic stem cells. *Genes Dev.* **26**, 1714-1728.

Cui, C.-H., Uyama, T., Miyado, K., Terai, M., Kyo, S., Kiyono, T. and Umezawa, A. (2007). Menstrual blood-derived cells confer human dystrophin expression in the murine model of Duchenne muscular dystrophy via cell fusion and myogenic transdifferentiation. *Mol. Biol. Cell* **18**, 1586-1594.

Efe, J. A., Hilcove, S., Kim, J., Zhou, H., Ouyang, K., Wang, G., Chen, J. and Ding, S. (2011). Conversion of mouse fibroblasts into cardiomyocytes using a direct reprogramming strategy. *Nat. Cell Biol.* **13**, 215-222.

Gafni, O., Weinberger, L., Mansour, A. A., Manor, Y. S., Chomsky, E., Ben-Yosef, D., Kalma, Y., Viukov, S., Maza, I., Zviran, A. et al. (2013). Derivation of novel human ground state naive pluripotent stem cells. *Nature* **504**, 282-286.

Han, D. W., Greber, B., Wu, G., Tapia, N., Araúzo-Bravo, M. J., Ko, K., Bernemann, C., Stehling, M. and Schöler, H. R. (2011). Direct reprogramming of fibroblasts into epiblast stem cells. *Nat. Cell Biol.* **13**, 66-71.

Han, D. W., Tapia, N., Hermann, A., Hemmer, K., Höing, S., Araúzo-Bravo, M. J., Zaehres, H., Wu, G., Frank, S., Moritz, S. et al. (2012). Direct reprogramming of fibroblasts into neural stem cells by defined factors. *Cell Stem Cell* **10**, 465-472.

Hanna, J., Markoulaki, S., Mitalipova, M., Cheng, A. W., Cassady, J. P., Staerk, J., Carey, B. W., Lengner, C. J., Foreman, R., Love, J. et al. (2009). Metastable pluripotent states in NOD-mouse-derived ESCs. *Cell Stem Cell* **4**, 513-524.

Hanna, J., Cheng, A. W., Saha, K., Kim, J., Lengner, C. J., Soldner, F., Cassady, J. P., Muffat, J., Carey, B. W. and Jaenisch, R. (2010). Human embryonic stem cells with biological and epigenetic characteristics similar to those of mouse ESCs. *Proc. Natl. Acad. Sci. USA* **107**, 9222-9227.

Hirano, K., Nagata, S., Yamaguchi, S., Nakagawa, M., Okita, K., Kotera, H., Ainscough, J. and Tada, T. (2012). Human and mouse induced pluripotent stem cells are differentially reprogrammed in response to kinase inhibitors. *Stem Cells Dev.* **21**, 1287-1298.

Hitoshi, S., Seaberg, R. M., Koscik, C., Alexson, T., Kusunoki, S., Kanazawa, I., Tsuji, S. and van der Kooy, D. (2004). Primitive neural stem cells from the mammalian epiblast differentiate to definitive neural stem cells under the control of Notch signaling. *Genes Dev.* **18**, 1806-1811.

Huang, P., He, Z., Ji, S., Sun, H., Xiang, D., Liu, C., Hu, Y., Wang, X. and Hui, L. (2011). Induction of functional hepatocyte-like cells from mouse fibroblasts by defined factors. *Nature* **475**, 386-389.

Ieda, M., Fu, J.-D., Delgado-Olguin, P., Vedantham, V., Hayashi, Y., Bruneau, B. G. and Srivastava, D. (2010). Direct reprogramming of fibroblasts into functional cardiomyocytes by defined factors. *Cell* **142**, 375-386.

Jiang, H., Shukla, A., Wang, X., Chen, W.-Y., Bernstein, B. E. and Roeder, R. G. (2011). Role for Dpy-30 in ES cell-fate specification by regulation of H3K4 methylation within bivalent domains. *Cell* **144**, 513-525.

Kim, J., Efe, J. A., Zhu, S., Talantova, M., Yuan, X., Wang, S., Lipton, S. A., Zhang, K. and Ding, S. (2011). Direct reprogramming of mouse fibroblasts to neural progenitors. *Proc. Natl. Acad. Sci. USA* **108**, 7838-7843.

Kumaki, Y., Oda, M. and Okano, M. (2008). QUMA: quantification tool for methylation analysis. *Nucleic Acids Res.* **36**, W170-W175.

Li, W., Wei, W., Zhu, S., Zhu, J., Shi, Y., Lin, T., Hao, E., Hayek, A., Deng, H. and Ding, S. (2009). Generation of rat and human induced pluripotent stem cells by combining genetic reprogramming and chemical inhibitors. *Cell Stem Cell* **4**, 16-19.

Li, W., Sun, W., Zhang, Y., Wei, W., Ambasudhan, R., Xia, P., Talantova, M., Lin, T., Kim, J., Wang, X. et al. (2011). Rapid induction and long-term self-renewal of primitive neural precursors from human embryonic stem cells by small molecule inhibitors. *Proc. Natl. Acad. Sci. USA* **108**, 8299-8304.

Lu, J., Liu, H., Huang, C. T.-L., Chen, H., Du, Z., Liu, Y., Sherafat, M. A. and Zhang, S.-C. (2013). Generation of integration-free and region-specific neural progenitors from primate fibroblasts. *Cell Rep.* **3**, 1580-1591.

Lujan, E., Chanda, S., Ahlenius, H., Sudhof, T. C. and Wernig, M. (2012). Direct conversion of mouse fibroblasts to self-renewing, tripotent neural precursor cells. *Proc. Natl. Acad. Sci. USA* **109**, 2527-2532.

Pang, Z. P., Yang, N., Vierbuchen, T., Ostermeier, A., Fuentes, D. R., Yang, T. Q., Citri, A., Sebastiano, V., Marro, S., Sudhof, T. C. et al. (2011). Induction of human neuronal cells by defined transcription factors. *Nature* **476**, 220-223.

Pereira, C.-F., Chang, B., Qiu, J., Niu, X., Papatsenko, D., Hendry, C. E., Clark, N. R., Nomura-Kitabayashi, A., Kovacic, J. C., Ma'ayan, A. et al. (2013). Induction of a hemogenic program in mouse fibroblasts. *Cell Stem Cell* **13**, 205-218.

Pfisterer, U., Kirkeby, A., Torper, O., Wood, J., Nelander, J., Dufour, A., Bjorklund, A., Lindvall, O., Jakobsson, J. and Parmar, M. (2011). Direct conversion of human fibroblasts to dopaminergic neurons. *Proc. Natl. Acad. Sci. USA* **108**, 10343-10348.

Qian, X., Shen, Q., Goderie, S. K., He, W., Capela, A., Davis, A. A. and Temple, S. (2000). Timing of CNS cell generation: a programmed sequence of neuron and glial cell production from isolated murine cortical stem cells. *Neuron* **28**, 69-80.

Ring, K. L., Tong, L. M., Balestra, M. E., Javier, R., Andrews-Zwilling, Y., Li, G., Walker, D., Zhang, W. R., Kreitzer, A. C. and Huang, Y. (2012). Direct reprogramming of mouse and human fibroblasts into multipotent neural stem cells with a single factor. *Cell Stem Cell* **11**, 100-109.

Sheng, C., Zheng, Q., Wu, J., Xu, Z., Wang, L., Li, W., Zhang, H., Zhao, X.-Y., Liu, L., Wang, Z. et al. (2012). Direct reprogramming of Sertoli cells into multipotent neural stem cells by defined factors. *Cell Res.* **22**, 208-218.

Smukler, S. R., Runciman, S. B., Xu, S. and van der Kooy, D. (2006). Embryonic stem cells assume a primitive neural stem cell fate in the absence of extrinsic influences. *J. Cell Biol.* **172**, 79-90.

Takahashi, K. and Yamanaka, S. (2006). Induction of pluripotent stem cells from mouse embryonic and adult fibroblast cultures by defined factors. *Cell* **126**, 663-676.

Takahashi, K., Tanabe, K., Ohnuki, M., Narita, M., Ichisaka, T., Tomoda, K. and Yamanaka, S. (2007). Induction of pluripotent stem cells from adult human fibroblasts by defined factors. *Cell* **131**, 861-872.

Theunissen, T. W., Powell, B. E., Wang, H., Mitalipova, M., Faddah, D. A., Reddy, J., Fan, Z. P., Maetzel, D., Ganz, K., Shi, L. et al. (2014). Systematic identification of culture conditions for induction and maintenance of naive human pluripotency. *Cell Stem Cell* **15**, 471-487.

Thier, M., Wörsdörfer, P., Lakes, Y. B., Gorris, R., Herms, S., Opitz, T., Seiferling, D., Quandel, T., Hoffmann, P., Nöthen, M. M. et al. (2012). Direct conversion of fibroblasts into stably expandable neural stem cells. *Cell Stem Cell* **10**, 473-479.

Tropepe, V., Hitoshi, S., Sirard, C., Mak, T. W., Rossant, J. and van der Kooy, D. (2001). Direct neural fate specification from embryonic stem cells: a primitive mammalian neural stem cell stage acquired through a default mechanism. *Neuron* **30**, 65-78.

Vierbuchen, T., Ostermeier, A., Pang, Z. P., Kokubu, Y., Südhof, T. C. and Wernig, M. (2010). Direct conversion of fibroblasts to functional neurons by defined factors. *Nature* **463**, 1035-1041.

Wada, T., Haigh, J. J., Ema, M., Hitoshi, S., Chaddah, R., Rossant, J., Nagy, A. and van der Kooy, D. (2006). Vascular endothelial growth factor directly inhibits primitive neural stem cell survival but promotes definitive neural stem cell survival. *J. Neurosci.* **26**, 6803-6812.

Wang, W., Yang, J., Liu, H., Lu, D., Chen, X., Zenonos, Z., Campos, L. S., Rad, R., Guo, G., Zhang, S. et al. (2011). Rapid and efficient reprogramming of somatic cells to induced pluripotent stem cells by retinoic acid receptor gamma and liver receptor homolog 1. *Proc. Natl. Acad. Sci. USA* **108**, 18283-18288.

Biology Open (2015) 4, 1595-1607 doi:10.1242/bio.013151

Wang, L., Wang, L., Huang, W., Su, H., Xue, Y., Su, Z., Liao, B., Wang, H., Bao, X., Qin, D. et al. (2013). Generation of integration-free neural progenitor cells from cells in human urine. *Nat. Methods* **10**, 84-89.

Wichterle, H., Lieberam, I., Porter, J. A. and Jessell, T. M. (2002). Directed differentiation of embryonic stem cells into motor neurons. *Cell* **110**, 385-397.

Ying, Q.-L., Wray, J., Nichols, J., Batlle-Morera, L., Doble, B., Woodgett, J., Cohen, P. and Smith, A. (2008). The ground state of embryonic stem cell self-renewal. *Nature* **453**, 519-523.

Yoo, A. S., Sun, A. X., Li, L., Shcheglovitov, A., Portmann, T., Li, Y., Lee-Messer, C., Dolmetsch, R. E., Tsien, R. W. and Crabtree, G. R. (2011). MicroRNA-mediated conversion of human fibroblasts to neurons. *Nature* **476**, 228-231.

SCIENTIFIC REPORTS

OPEN

Glycolipid dynamics in generation and differentiation of induced pluripotent stem cells

Received: 23 October 2014
Accepted: 07 September 2015
Published: 19 October 2015

Takuma Ojima[1,2,*], Eri Shibata[1,2,*], Shiho Saito[1,2], Masashi Toyoda[1,3], Hideki Nakajima[1], Mayu Yamazaki-Inoue[1], Yoshitaka Miyagawa[1], Nobutaka Kiyokawa[1], Jun-ichiro Fujimoto[1], Toshinori Sato[2] & Akihiro Umezawa[1]

Glycosphingolipids (GSLs) are glycoconjugates that function as mediators of cell adhesion and modulators of signal transduction. Some well-defined markers of undifferentiated human embryonic stem cells (hESCs) and human induced pluripotent stem cells (hiPSCs) are glycoconjugates, such as SSEA-3, SSEA-4, TRA-1-60 and TRA-1-81. However, Comprehensive GSL profiles of hiPSCs have not yet been elucidated. The global images of GSLs from the parental cells, hiPSCs, and differentiated cells revealed that there are parental cell-independent specific glycolipids, including Globo H (fucosyl-Gb5Cer) and H type1 antigen (fucosyl-Lc4Cer) that are novel markers for undifferentiated hiPSCs. Interestingly, undifferentiated hiPSCs expressed H type 1 antigen, specific for blood type O, regardless of the cells' genotypes. Thus, in this study, we defined the dynamics of GSL remodeling during reprogramming from parental cell sets to iPSC sets and thence to iPSC-neural cells.

When the technology to generate human iPS cells (hiPSCs) first became available[1,2], immediate attention was placed on their potential for use in cell-based transplantation. Both iPSCs (differentiated *in vitro*) and embryonic stem cells (ESCs) can provide an unlimited source of useful cell types for transplantation. The use of hiPSCs is desirable because they lack the substantial ethical concern of cellular origin that plagues ESCs. The fact that hiPSCs are autologous for patients is another advantage in transplantation. However, one of the major drawbacks for transplantation of iPSCs is their labile/variable state due to epigenetic dynamics during cultivation and their carcinogenic potential due to oncogene infection[3]. Soon after hiPSC technology was developed, researchers began to realize an additional and possibly greater value for the cells to help elucidate the causes of disease. hiPSCs can be generated from skin biopsies or blood samples of patients, and can differentiate *in vitro* into cell types that are not easily accessible from patients.

The glycans expressed on the cell membrane differ among cell lines, and participate in development, differentiation, activation, inflammation, and malignant transformation[4-6]. Therefore, glycan profiling, in addition to genomic and epigenetic profiling, may provide valuable information about the signal transduction pathways during these events, and in fact has already shown promise in the fields of reproductive medicine and oncology[7,8]. Antibodies are commonly employed to recognize glycans in cells, and lectins, which recognize specific glycan epitopes, have been used for blood-group typing, tissue staining, lectin-probed blotting and flow cytometry. Recently, a lectin microarray enabled discriminate glycan profiling between different cell lines by ultrasensitive detection of multiplex lectin-glycan interactions[9]. In addition to the use of antibodies and lectins, the saccharide primer method has been used to screen essential cell-surface carbohydrates[10,11]. Biochemical approaches such as liquid chromatography-tandem

[1]National Research Institute for Child Health and Development, Tokyo, 157-8535, Japan. [2]Department of Biosciences and Informatics, Keio University, Kanagawa, 223-8522, Japan. [3]Department of Research Team for Geriatric Medicine, Tokyo Metropolitan Institute of Gerontology, Tokyo, 173-0015, Japan. *These authors contributed equally to this work. Correspondence and requests for materials should be addressed to A.U. (email: umezawa@1985.jukuin.keio.ac.jp)

mass spectrometry (LC-MS) have also been used to analyze carbohydrate structures for identification of cell types and for evidence of transformation[12-14]. The comprehensive analysis with LC-MS also revealed specific glycan structures in pluripotent stem cells and somatic cells[15].

Stem cells have the ability to divide, self-renew and to differentiate into various cell types. Stem cells have varying degrees of differentiation potential: (a) totipotency (the ability to form the embryo and placental cells), as seen in fertilized eggs (zygotes); (b) pluripotency (the ability to differentiate into almost all cells that arise from the three germ layers), as found in hESCs and hiPSCs; (c) multipotentiality (the capability of producing a limited range of differentiated cell lineages upon their location), as demonstrated by most tissue-based stem cells; and (d) unipotentiality (the ability to generate one cell type), as exhibited by epidermal stem cells and the spermatogonial cells of the testis. That is, a hierarchy of stem cells exists. In addition, ESCs show variation in differentiation propensity. iPSCs, another type of pluripotent stem cell, have been generated from somatic cells of different origins by retroviral transduction of four transcription factors[1,2]. The established iPSCs have a wider variety of differentiation ability and gene expression than ESCs. However, a small proportion of these stem cells sometimes show spontaneous differentiation during serial passage. Therefore, in order to realize the full potential for iPSCs in cell therapy and drug discovery, it is necessary to monitor the status of these stem cells and to define their exact stage during processes of growth and/or differentiation.

Carbohydrate epitopes are often used as markers for definition and characterization of stem cells. Stage-specific embryonic antigens such as SSEA-3, SSEA-4, TRA-1-60 and TRA-1-81 are also used as markers for the undifferentiated state of human ESCs (hESCs) and hiPSCs[1]. Glycosphingolipids (GSLs) expressed in hESCs have been examined by immunofluorescence, flow cytometry and mass spectrometry[16,17]. GSLs such as Gb5Cer (SSEA-3), sialyl-Gb5Cer (SSEA-4), fucosyl-Gb5Cer (Globo H), and IV fucosyl-Lc4Cer (H type 1 antigen), have been identified in hESCs. In this study, we investigated the hiPSC-specific GSLs that were induced and highly expressed at the earliest stages of iPSCs generation and then down-regulated upon differentiation. We propose that the glycolipid dynamics during generation and differentiation of iPSCs will lead to a better understanding of cellular reprogramming.

Results

Analysis of GSLs in MRC-5 cells and UtE cells. GSLs in MRC-5 and UtE cells were analyzed using LC-MS (Fig. 1A,C); the results are shown in Table 1. Though the fatty acid length of ceramide varied from C14:0 through C26:0, only the results for GSLs with C16:0 and C24:0 are indicated in Table 1. Analyses of MS/MS spectra revealed that the four neutral GSLs were deduced to be GlcCer, LacCer, Gb3Cer, Gb4Cer, and the five acidic GSLs were deduced to be GM3, GM2, GM1, GD3, and GD1a/GD1b for both MRC-5 cells and UtE cells (Supplemental Table S1A, S1B). The neutral GSLs were detected as Hex-Cer, Hex-Hex-Cer, and Hex-Hex-Hex-Cer, HexNAc-Hex-Hex-Hex-Cer by MS/MS analysis. Though the neutral GSLs have isomers depending on the variety of monosaccharide, their structures were deduced to be GlcCer, LacCer, Gb3Cer, Gb4Cer because they are major GSLs and detected even in hESCs[18]. However, since GalCer and galabiose as isomers of GlcCer and LacCer have been detected in hESCs[18], existence of other isomers in hiPSCs could not be excluded.

Analysis of GSLs in hiPSCs. Undifferentiated hiPSCs induced from MRC-5 and UtE cells were identified by immunostaining using antibodies against SSEA-4, TRA-1-60, NANOG, OCT3/4, and SOX2 (Supplemental Figure S1). GSLs of the hiPSCs were analyzed using LC–MS. Though the fatty acid length of ceramide ranged from C16:0 through C26:0, the major fatty acids were C16:0 and C18:0. When the ceramide was d18:1/C16:0, extracted-ion chromatogram (EIC) of m/z at 734.5, 896.6, 1058.6, 1261.7, 1407.8, 1423.8, 1569.8 as $[M+Cl]^-$, 1151.7, 1354.8, 1516.8, 1678.8 as $[M\text{-}H]^-$ and 720.9 as $[M\text{-}2H]^{2-}$ were detected for both MRC-iPSCs and UtE-iPSCs. Thus, two kinds of hiPSCs induced from the different parental cells showed identical GSL composition; there was no significant difference between MRC-iPSCs and UtE-iPSCs. Eight neutral GSLs and five acidic GSL were detected. By MS/MS analysis (Supplemental Table S1C and S1D), the eight neutral GSLs were deduced to be GlcCer (m/z 734.5), LacCer (m/z 896.6), Gb3Cer (m/z 1058.6), Gb4Cer/(n)Lc4Cer (m/z 1261.7), IV fucosyl-(n)Lc4Cer (m/z 1407.8), Gb5Cer (m/z 1423.8), fucosyl-Gb5Cer (m/z 1569.8). The five acidic GSLs were deduced to be GM3(m/z 1151.7), GM2 (m/z 1354.8), GM1 (m/z 1516.8), GD3 (m/z 720.9) and sialyl-Gb5Cer (m/z 1678.8). Of note, Gb5Cer, sialyl-Gb5Cer, fucosyl-Gb5Cer and IV fucosyl-(n)Lc4Cer were detected in iPSCs, but not in parental cells. The sequence of Gb5Cer deduced by MS/MS analysis was Hex-HexNAc-Hex-Hex-Hex-Cer (Fig. 2A,D). Using the same methodology, the sequence of sialyl-Gb5Cer was NeuAc-Hex-HexNAc-Hex-Hex-Hex-Cer (Fig. 2D); IV fucosyl-(n)Lc4Cer was Fuc-Hex-HexNAc-Hex-Hex-Cer (Fig. 2B,D) and the sequence of fucosyl-Gb5Cer was Fuc-Hex-HexNAc-Hex-Hex-Hex-Cer (Fig. 2C,D). Though those sequences have isomers, the structures were deduced from the MS/MS analysis and immunocytochemical analysis described later. They were major GSLs synthesized by biosynthetic pathways expressed in hESCs[16-19]. This is the first time that the structures for Gb5Cer, sialyl-Gb5Cer, fucosyl-Gb5Cer, and IV fucosyl-(n) Lc4Cer were identified in undifferentiated hiPSCs.

Analysis of GSLs in NSC differentiated from hiPSCs. To investigate the alteration of GSLs during differentiation of hiPSCs, hiPSCs were differentiated to neural stem cells (NSCs) according to the standard protocol. The differentiation of MRC- and UtE-iPSCs to NSCs was confirmed by immunostaining

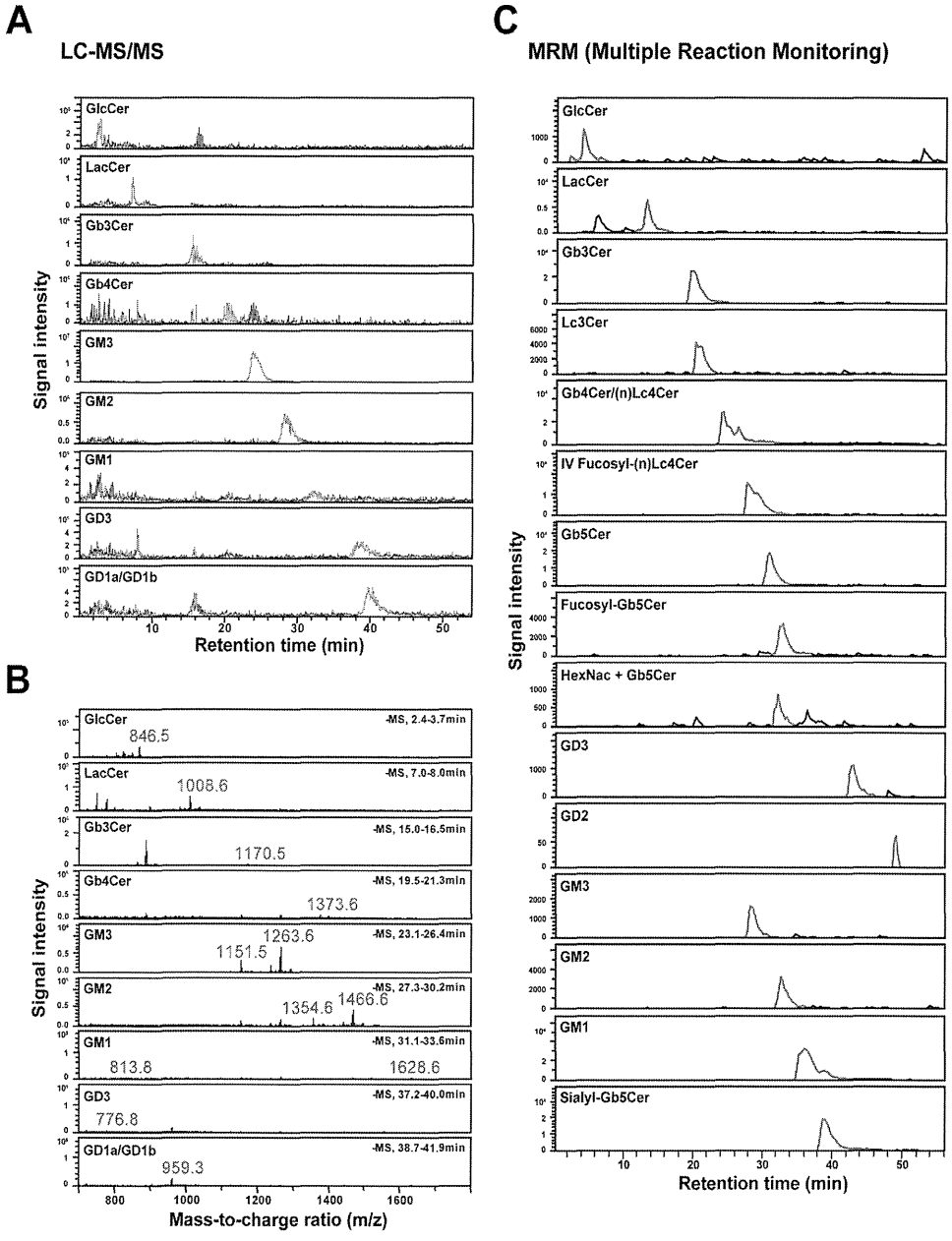

Figure 1. LC-MS/MS analysis on GSLs of iPS cells and their parental cells. (**A**–**C**) LC chromatogram and mass spectrum on iPS cells and parental MRC-5 cells. (**A**) LC chromatogram of MRC-5 cells. (**B**) Mass spectrum of MRC-5 cells. (**C**) LC chromatogram of MRCiPS#25 cells.

using antibodies against SOX1, SOX2, PAX6, NESTIN, and TUJ-1 as NSC markers (Supplemental Figure S2), and OCT3/4, NANOG, SOX2, SSEA-3, SSEA-4, TRA-1-60 as iPS markers. Moreover, the expression of NSC markers such as SOX1, PAX6, HES5, NOTCH, and GPM6A were confirmed by RT-PCR. These results confirmed the successful differentiation from iPSCs to NSCs. GSLs of NSCs was analyzed by LC-MS. Though the length of the fatty acid in ceramide ranged from C16:0 through C26:0, the major fatty acids were C16:0 and C24:0. When ceramide was d18:1/C16:0, EIC of m/z at 734.5, 896.6, 1058.6, 1099.7, 1261.7, 1407.8 as $[M+Cl]^-$, 1151.7, 1354.8, 1516.8 as $[M\text{-}H]^-$, and 720.9, 822.4, 903.5 as $[M\text{-}2H]^{2-}$ were detected. By MS/MS analysis (Supplemental Table S2A, S2B), the six neutral GSLs were deduced to be GlcCer (m/z 734.5), LacCer (m/z 896.6), Gb3Cer (m/z 1058.6), Lc3Cer (m/z 1099.7), (n)Lc4Cer (m/z 1261.7), III fucosyl-(n)Lc4Cer (m/z 1407.8); and the six acidic GSLs were deduced to be GM3 (m/z 1151.7), GM2 (m/z 1354.8), GM1 (m/z 1516.8), GD3 (m/z 720.9), GD2 (m/z 822.4), GD1a /GD1b (m/z 903.5). The sequence of III fucosyl-(n)Lc4Cer deduced by MS/MS analysis is Hex-(Fuc-)HexNAc-Hex-Hex-Cer. The Gb5Cer, sialyl-Gb5Cer, fucosyl-Gb5Cer, and IV fucosyl-(n)Lc4Cer expressed in hiPSCs were not detected in NSCs, while III fucosyl-(n)Lc4Cer was detected. There was no significant difference between the NSCs differentiated from MRC-iPSCs and UtE-iPSCs.

Analysis of GSL in embryoid body (EB) outgrowth differentiated from iPSCs. The alteration of GSLs upon differentiation from hiPSCs to EB outgrowth was also investigated. Differentiation of

Proposed GSLs	Cer	Ion Type	Calculated Mass (m/z)	Observed Mass (m/z)	
				MRC-5	UtE
GlcCer	d18:1/24:0	$[M+Cl]^-$	846.7	848.4	847.4
	d18:1/16:0	$[M+Cl]^-$	735.1	N.D.	N.D.
LacCer	d18:1/24:0	$[M+Cl]^-$	1008.7	1008.4	1008.4
	d18:1/16:0	$[M+Cl]^-$	896.6	896.4	N.D.
Gb3Cer	d18:1/24:0	$[M+Cl]^-$	1170.8	1170.4	1170.9
	d18:1/16:0	$[M+Cl]^-$	1058.6	1059.1	1058.9
Gb4Cer	d18:1/24:0	$[M+Cl]^-$	1373.8	1372	N.D.
	d18:1/16:0	$[M+Cl]^-$	1261.7	N.D.	1261.9
GM3	d18:1/24:0	$[M-H]^-$	1263.8	1263.4	1263.3
	d18:1/16:0	$[M-H]^-$	1151.7	1152.1	1152.4
GM2	d18:1/24:0	$[M-H]^-$	1466.9	1466.9	1466.6
	d18:1/16:0	$[M-H]^-$	1354.8	1355.4	1355.1
GM1	d18:1/24:0	$[M-H]^-$	1629	N.D.	1628.4
	d18:1/16:0	$[M-H]^-$	1516.8	1517.1	1517.7
GD3	d18:1/24:0	$[M-2H]^{2-}$	777	777	776.8
	d18:1/16:0	$[M-2H]^{2-}$	720.9	720.9	720.9
GD1a	d18:1/24:0	$[M-2H]^{2-}$	959.5	959.2	959.2
	d18:1/16:0	$[M-2H]^{2-}$	903.5	904.9	903.8

Table 1. GSLs detected in parental cells. N.D. means "not detected".

MRC-iPSCs and UtE-iPSCs to tridermic EB cells was confirmed by immunostaining with antibodies against Tuj-1, αSMA and AFP (Supplemental Figure S3A). GSLs of EB outgrowth were analyzed by LC-MS. Though the length of fatty acid in ceramide varied from C16:0 through C26:0, major fatty acids were C16:0 and C24:0, and were similar to the fatty acids found in NSCs. When ceramide was d18:1/C16:0, EIC of m/z at 734.5, 896.6, 1058.6, 1099.7, 1261.7, 1407.8 as $[M+Cl]^-$, and 1151.7, 1354.8, 1516.8 as $[M-H]^-$, and 720.9, 822.4, 903.5 as $[M-2H]^{2-}$, were detected. By MS/MS analysis (Supplemental Table S2C, S2D), the six neutral GSLs were deduced to be GlcCer (m/z 734.5), LacCer (m/z 896.6), Gb3Cer (m/z 1058.6), Lc3Cer (m/z 1099.7), (n)Lc4Cer (m/z 1261.7), III fucosyl-(n)Lc4Cer (m/z 1407.8), and the six acidic GSLs were deduced to be GM3 (m/z 1151.7), GM2 (m/z 1354.8), GM1 (m/z 1516.8), GD3, (m/z 720.9) GD2 (m/z 822.4), and GD1a/GD1b (m/z 903.5). There were no significant differences between the EB outgrowths differentiated from MRC-iPSCs and UtE-iPSCs. Moreover, these GSLs in EB outgrowths were similar to those found in NSCs. The analysis of GSL immediately after EB formation was also carried out. The detected GSLs were a mixture of the GSLs observed in hiPSCs and EB outgrowth.

Immunocytochemical and flow cytometric analysis of parental cells, hiPSCs, NSCs, and EB outgrowth. The results of GSL analysis in parental cells, hiPSCs, NSCs, and EB outgrowth are summarized in Table 2. In addition to Gb5Cer and sialyl-Gb5Cer corresponding to SSEA-3 and SSEA-4, which are markers for undifferentiated hiPSCs, fucosyl-Gb5Cer and IV fucosyl-(n)Lc4Cer corresponding to Globo H and H type 1 antigen, were specifically expressed only in undifferentiated hiPSCs. To confirm the GSL analysis, immunocytochemical analysis and flow cytometric analysis using antibodies against SSEA-4, Globo H, H type1 antigen, and SSEA-1 were carried out. Immunocytochemical analyses showed that MRC-iPSCs were positive for Globo H and H type1 antigen (Fig. 3A), and NSCs and EB-outgrowth were positive for SSEA-1. Flow cytometric analyses also revealed that the MRC-iPSCs were positive for Globo H, H type1 antigen, and SSEA-3, and were negative for SSEA-1. NSCs were positive for SSEA-1 (Fig. 3B). Similar results were also obtained for iPSCs, NSC, and EB-outgrowth derived from UtE cells as parent cells (Supplemental Figure S3B, S4). These results suggest that fucosyl-(n)Lc4Cer detected in iPSCs was IV fucosyl-Lc4Cer corresponding to H type 1 antigen, and fucosyl-(n) Lc4Cer detected in NSCs and EB outgrowth was III fucosyl-nLc4Cer corresponding to SSEA-1. Time-dependent expression of SSEA-4, Globo H and H type 1 antigen were also measured during the differentiation process of iPSCs to NSCs. These antigens were no longer expressed after cultivation of the cells in the NSC differentiation medium for 6 days followed by cultivation in NSC maintenance medium for 3 days (Fig. 3C).

Determination of ABO genotyping. Because both MRC-iPSCs and UtE-iPSCs express H antigen (blood type O), ABO genotyping of both cell types was carried out by two different methods[20,21]. Both the allele-specific primer method and sequencing of the ABO transferase gene revealed that MRC-5 cells

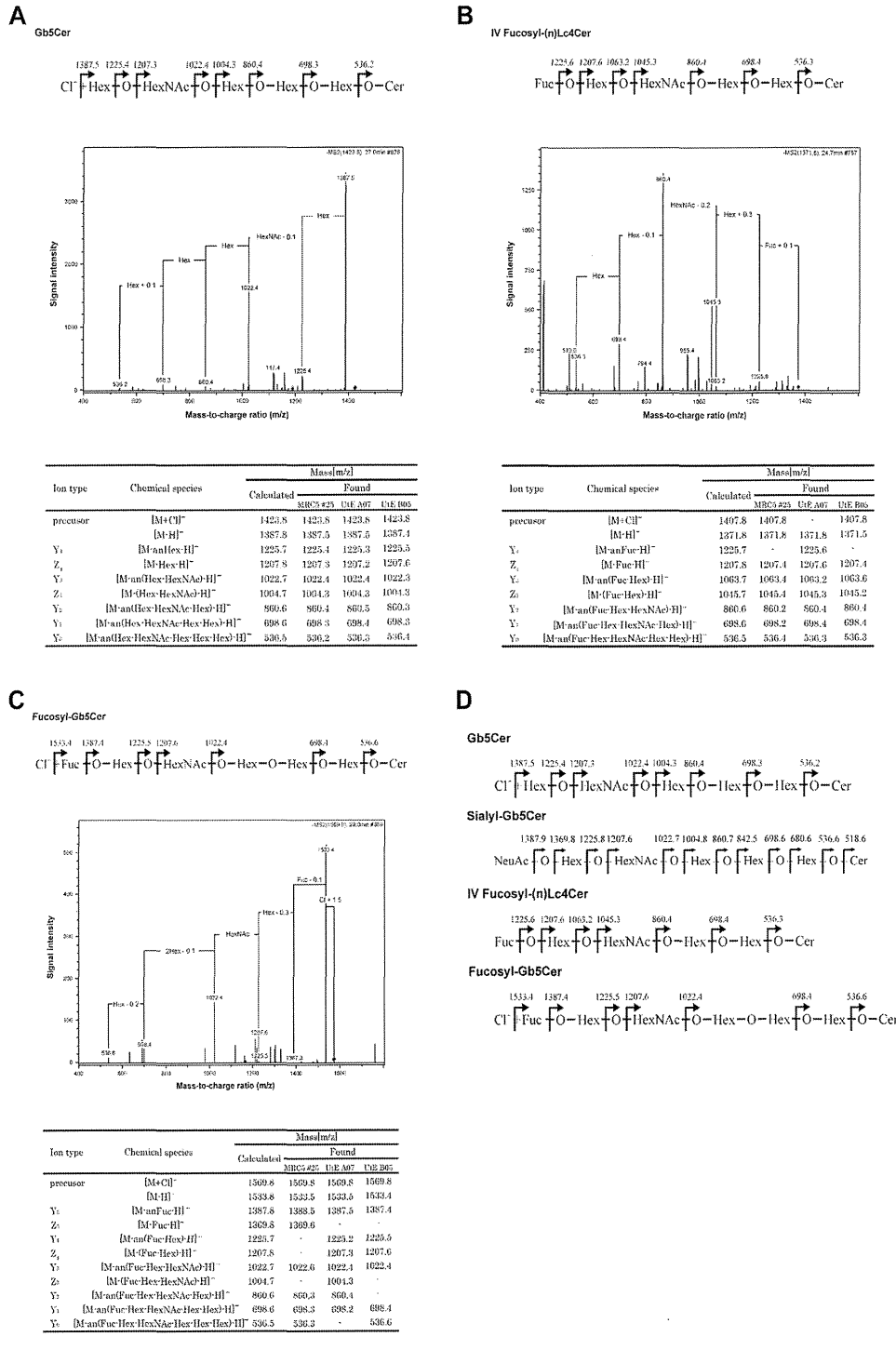

Ion type	Chemical species	Mass[m/z] Calculated	Found MRC5 #23	Found UtE A07	Found UtE B05
precusor	$[M+Cl]^-$	1423.8	1423.8	1423.8	1423.8
	$[M-H]^-$	1387.8	1387.5	1387.5	1387.4
Y_1	$[M-anHex-H]^-$	1225.7	1225.4	1225.3	1225.5
Z_2	$[M-Hex-H]^-$	1207.8	1207.3	1207.2	1207.6
Y_2	$[M-an(Hex-HexNAc)-H]^-$	1022.7	1022.4	1022.4	1022.3
Z_1	$[M-(Hex-HexNAc)-H]^-$	1004.7	1004.3	1004.3	1004.3
Y_3	$[M-an(Hex-HexNAc-Hex)-H]^-$	860.6	860.4	860.5	860.3
Y_4	$[M-an(Hex-HexNAc-Hex-Hex)-H]^-$	698.6	698.3	698.4	698.3
Y_5	$[M-an(Hex-HexNAc-Hex-Hex-Hex)-H]^-$	536.5	536.2	536.5	536.4

Ion type	Chemical species	Mass[m/z] Calculated	Found MRC5 #23	Found UtE A07	Found UtE B05
precusor	$[M+Cl]^-$	1407.8	1407.8	-	1407.8
	$[M-H]^-$	1371.8	1371.8	1371.8	1371.5
Y_1	$[M-anFuc-H]^-$	1225.7	-	1225.6	-
Z_2	$[M-Fuc-H]^-$	1207.8	1207.4	1207.6	1207.4
Y_2	$[M-an(Fuc-Hex)-H]^-$	1063.7	1063.4	1063.2	1063.6
Z_3	$[M-(Fuc-Hex)-H]^-$	1045.7	1045.4	1045.3	1045.2
Y_3	$[M-an(Fuc-Hex-HexNAc)-H]^-$	860.6	860.2	860.4	860.4
Y_4	$[M-an(Fuc-Hex-HexNAc-Hex)-H]^-$	698.6	698.2	698.4	698.4
Y_5	$[M-an(Fuc-Hex-HexNAc-Hex-Hex)-H]^-$	536.5	536.4	536.3	536.3

Ion type	Chemical species	Mass[m/z] Calculated	Found MRC5 #25	Found UtE A07	Found UtE B05
precusor	$[M+Cl]^-$	1569.8	1569.8	1569.8	1569.8
	$[M-H]^-$	1533.8	1533.5	1533.5	1533.4
Y_1	$[M-anFuc-H]^-$	1387.8	1388.5	1387.5	1387.4
Z_3	$[M-Fuc-H]^-$	1369.8	1369.6	-	-
Y_4	$[M-an(Fuc-Hex)-H]^-$	1225.7	-	1225.2	1225.5
Z_4	$[M-(Fuc-Hex)-H]^-$	1207.8	-	1207.3	1207.6
Y_2	$[M-an(Fuc-Hex-HexNAc)-H]^-$	1022.7	1022.6	1022.4	1022.4
Z_2	$[M-(Fuc-Hex-HexNAc)-H]^-$	1004.7	-	1004.3	-
Y_3	$[M-an(Fuc-Hex-HexNAc-Hex)-H]^-$	860.6	860.3	860.4	-
Y_4	$[M-an(Fuc-Hex-HexNAc-Hex-Hex)-H]^-$	698.6	698.3	698.2	698.4
Y_5	$[M-an(Fuc-Hex-HexNAc-Hex-Hex-Hex)-H]^-$	536.5	536.3	-	536.6

Figure 2. GSLs of iPS cells and their parental cells. (**A**–**C**) MS/MS spectrum of iPS cells. (**A**) Gb5Cer. (**B**) IV Fucosyl-(n)Lc4Cer. (**C**) Fucosyl-Gb5Cer. (**D**) Sequences of Gb5Cer, sialyl-Gb5Cer, V fucosyl-(n) Lc4Cer and fucosyl-Gb5Cer deduced by MS/MS analysis.

and UtE cells carried genotypes for blood types O and A, respectively (Fig. 4). These results imply that iPSCs express H antigen (blood type O) when in the undifferentiated state, irrespective of blood group antigen genotype.

Genetic alteration of glycan biosynthesis during iPSC generation. The biosynthetic pathways for the GSLs observed in these studies are shown in Fig. 5A–D and Table 2. The major glycosyltransferase genes related to synthesis of the GSLs are also indicated (Fig. 5A–D). In Table 2, several GSLs were not detected in the present study. However, we could not exclude the possibility of the presence of the GSLs. To determine whether the proposed GSL synthetic pathways were actually functional in parental cells and hiPSCs, quantitative RT-PCR was carried out for the glycosyltransferase genes ST3GAL5, A4GALT, B3GNT5, B4GALNT1, B3GALT5, FUT1 and FUT2. The copy numbers of those genes ranged from 10^3–10^6/1μg RNA. The relative values of iPS/parent cells were evaluated for each gene (Fig. 5E).

Proposed GSLs	Parental cells		iPSC		EB-outgrowth		NSC	
	MRC-5	UtE	MRC-5	UtE	MRC-5	UtE	MRC-5	UtE
GlcCer	+	N.D.	+	+	+	+	+	+
LacCer	N.D.	+	+	+	+	+	+	+
Gb3Cer	+	+	+	+	+	+	+	+
Gb4Cer	+	+	+	+	+	+	+	+
Gb5Cer	N.D.	N.D.	+	+	N.D.	N.D.	N.D.	N.D.
Fucosyl-Gb5Cer	N.D.	N.D.	+	+	N.D.	N.D.	N.D.	N.D.
HexNAc+ Gb5Cer	N.D.	N.D.	N.D.	N.D.	N.D.	N.D.	N.D.	N.D.
Sialyl-Gb5Cer	N.D.	N.D.	+	+	N.D.	N.D.	N.D.	N.D.
Lc3Cer	N.D.	N.D.	+	+	+	+	+	+
(n)Lc4Cer	N.D.	N.D.	+	+	+	+	+	+
IV Fucosyl-(n)Lc4Cer	N.D.	N.D.	+	+	N.D.	N.D.	N.D.	N.D.
III Fucosyl-(n)Lc4Cer	N.D.	N.D.	N.D.	N.D.	+	+	+	+
GM3	+	+	+	+	+	+	+	+
GM2	+	+	+	+	+	+	+	+
GM1	+	+	+	+	+	+	+	+
GD3	+	+	+	+	+	+	+	+
GD2	N.D.	N.D.	+	N.D.	+	+	+	+
GD1a/GD1b	+	+	N.D.	N.D.	+	+	+	+

Table 2. GSLs detected in parental cells, iPSCs, EB-outgrowth, and neural stem cells. N.D. means "not detected".

Expression of ST3GAL5 and B4GALNT1, which function in the biosynthesis of ganglio-series GM3 and GM2, respectively, were significantly decreased after iPSC generation. The expression of B3GNT5, responsible for the biosynthesis of Lc3Cer, was up-regulated in MRC-iPSCs, but was down-regulated in UtE-iPSCs. In contrast, A4GALT, which functions in globo-series GSL biosynthesis, was down-regulated in MRC-iPSCs, but in UtE-iPSCs, it was up-regulated. Based on these results, the increase in globo- and lacto/neolacto-series GSLs in hiPSCs was a result of the decreased expression of the GM3 synthase gene ST3GAL5. Though the predominant glycan synthetic pathway in the parental cells is for ganglio-series GSLs, the predominant pathways in hiPSCs switched to the globo- and lacto-series GSLs, due to the large decrease in GM3 synthase. Additionally, FUT1 and FUT2, which are related to biosynthesis of Globo H, H type1 antigen and other H antigens, were upregulated in hiPSCs. Therefore, we conclude that the expression of fucosyl-Gb5Cer and IV fucosyl-(n)Lc4Cer in hiPSCs were influenced by both the increase of FUT1/FUT2 and the increase in globo- and lacto/neolacto-series GSL biosynthesis. Accordingly, three kinds of MRC-iPSCs and two kinds of UtE-iPSCs were prepared in order to examine the expression of these glycosyltransferase genes, and the results were similar for all five iPSCs (Supplemental Figure S5).

Glycan biosynthesis-related genes in iPSC-derived NSCs and EB outgrowth. To investigate expression of glycan biosynthesis-related genes during differentiation from iPSCs to NSCs and during EB outgrowth, quantitative RT-PCR for the genes ST3GAL5, A4GALT, B3GNT5, B4GALNT1, B3GALT5, FUT1 and FUT2 was carried out in NSCs and EB-outgrowth (Fig. 5F,G). ST3GAL5 and B4GALNT1, responsible for biosynthesis of ganglio-series, increased in NSCs and EB outgrowth that had been differentiated from MRC-iPSCs and UtE-iPSCs. In contrast, A4GALT, involved in biosynthetic pathway of globo-series GSLs such as Gb5Cer, sialyl-Gb5Cer, and fucosyl-Gb5Cer, was down-regulated. B3GNT5, the Lc3Cer synthase gene, showed an increase in expression during differentiation of hiPSCs to EB growth and NSC, FUT1/FUT2 expression increased in EB outgrowth, but not in NSCs.

Discussion

GSLs presented on the surface of mammalian cells participate many important biological functions, but analysis of the expression of GSLs in hESCs has only been reported recently[16-18]. Though hESCs and hiPSCs are considered to be identical in many aspects including cell surface markers, expression of GSLs in hiPSCs has not been reported. In the present study, glycolipid dynamics during generation and differentiation of hiPSCs was investigated using LC-MS. Dynamic gene expression and epigenetic changes continues for more than 50 weeks after iPSC generation[22,23]. In our study, global images of GSLs determined by LC-MS clearly showed drastic alterations immediately after iPS generation (Table 2). Several GSLs were not detected in the present study. In some cases, the GSLs might not be detected because the measurement was beyond the limits of sensitivity. The lipid extracts without alkaline hydrolysis were also

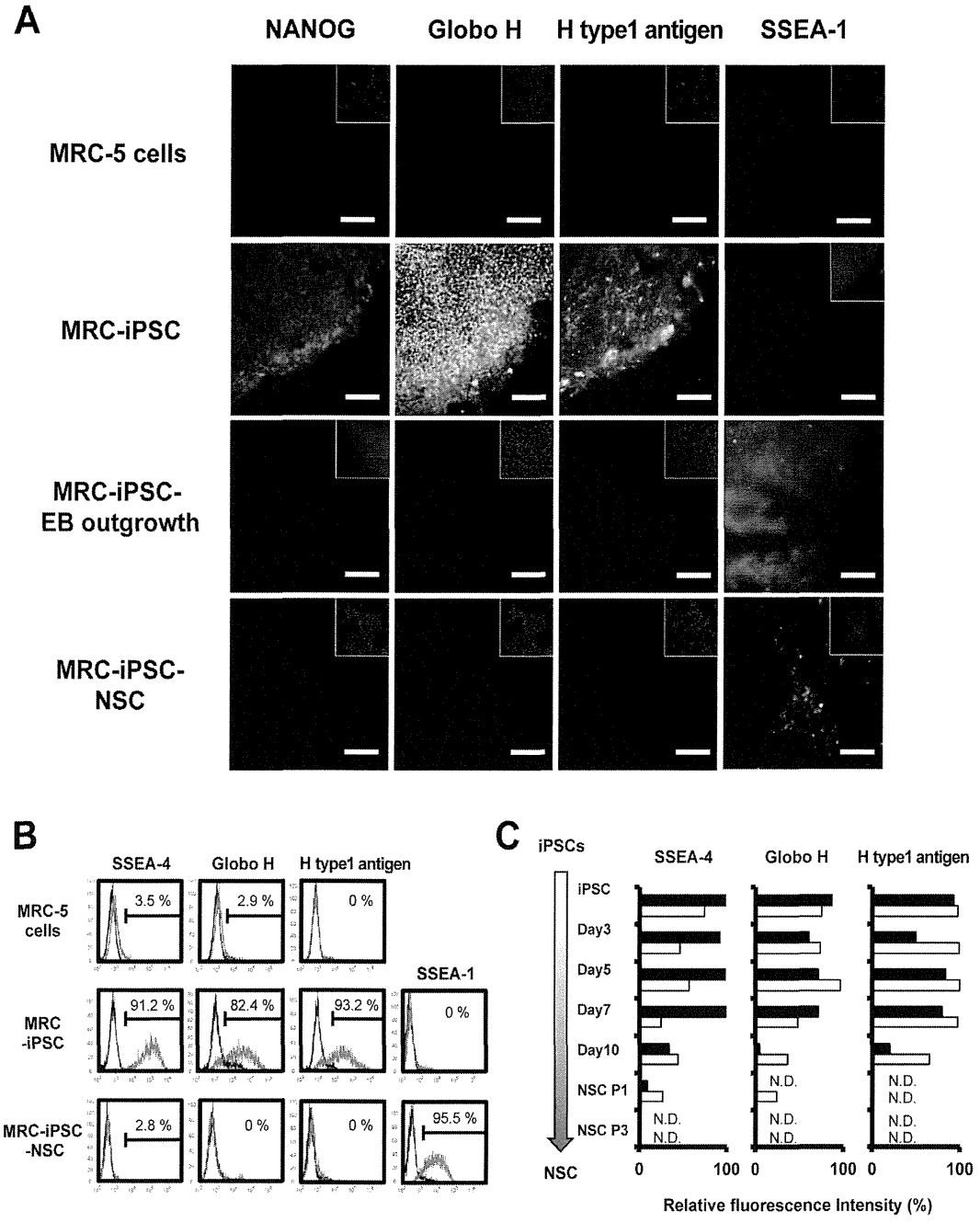

Figure 3. GSL expression in iPSCs, their parental cells and iPSC-NSCs. (**A**) Immunocytochemical analyses of NANOG, Globo H, H type1 antigen, and SSEA-1 in MRC-5, MRC-iPSCs, MRC-iPSC-EB outgrowth, and MRC-iPSC-NSCs. Inserted images are nuclear staining by DAPI. Scale bar is 100 μm. (**B**) Flow cytometric analyses of GSLs in MRC-5, MRC-iPSCs, and MRC-iPSC-NSCs. SSEA-4, Globo H, H type1 antigen and SSEA-1 were analyzed using GSL-specific antibodies versus the isotype controls. Cells stained with specific antibodies are shown in red, and isotype antibodies are shown in black. (**C**) Time course analyses by flow cytometry of SSEA-4, Globo H, and H type1 antigen during the process of differentiation from iPSCs to NSCs. Black columns represent MRC-iPSCs and white columns, UtE-iPSCs. N.D. is "not detected".

analyzed by LC-MS to eliminate possibility of GSL hydrolysis. However, no differences in the variety of GSLs between the lipid extracts with or without alkaline hydrolysis were observed in the present study. We could not determine structure of some GSLs due to lack of, or low levels of GSLs ("not detected" in Table 2). The GSL panel in Table 2 indicates the distinctive expression of globo-series and lacto/neolacto-series in undifferentiated iPSCs, compared to parental somatic cells and differentiated forms of hiPSCs. Consistent correlation between the expression levels of GSLs and the corresponding glycosyltransferases strongly suggests that regulation of glycosyltransferase genes are the direct cause of glycolipid dynamics during generation of iPSCs. The significant down-regulation of ST3GAL5 and B4GALNT1 correlated with the biosynthesis of ganglio-series GSLs and influenced the increase of globo and lacto/

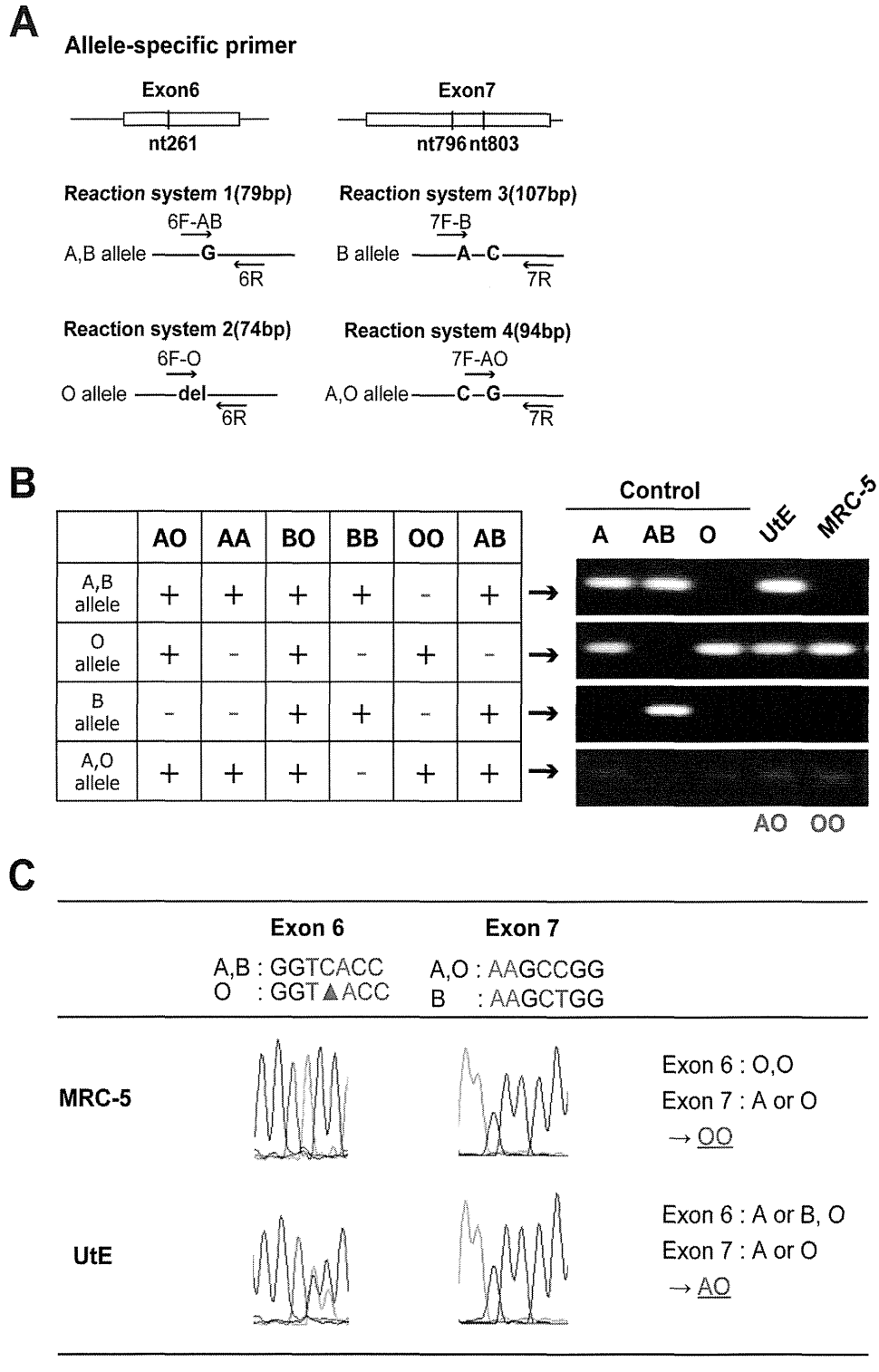

Figure 4. Determination of ABO genotypes. (**A**) Allele-specific primers for the ABO transferase gene. (**B**) ABO genotyping for MRC and UtE cells. Each RT-PCR gel was electrophoresed at the same time. The gels were cropped to show the corresponding bands clearly. (**C**) Sequence analysis of the genes for ABO system transferase.

neolacto-series GSLs. Up-regulation of A4GALT in UtE-iPSCs and B3GNT5 in MRC-iPSCs also resulted in an increase of globo and lacto/neolacto-series GSLs. Gaglio-, globo-, and lacto/neolacto-series GSLs were synthesized from lactosylceramide as a precursor. Since GM3, Gb3Cer, and Lc3Cer are competitively biosynthesized in cells, down-regulation of GM3 biosynthesis would induce the up-regulation of the biosynthesis of Gb3Cer and Lc3Cer.

SSEA-3 and SSEA-4 are markers of undifferentiated hiPSCs. In our study, the structures of GSLs corresponding to SSEA-3 and SSEA-4 were deduced to be Gb5Cer and sialyl-Gb5Cer, respectively, by MS/MS analysis. In addition to SSEA-3 and SSEA-4, Globo H was also detected by immunocytochemical analysis. The structure of Globo H was deduced to be fucosyl Gb5Cer, which is synthesized by

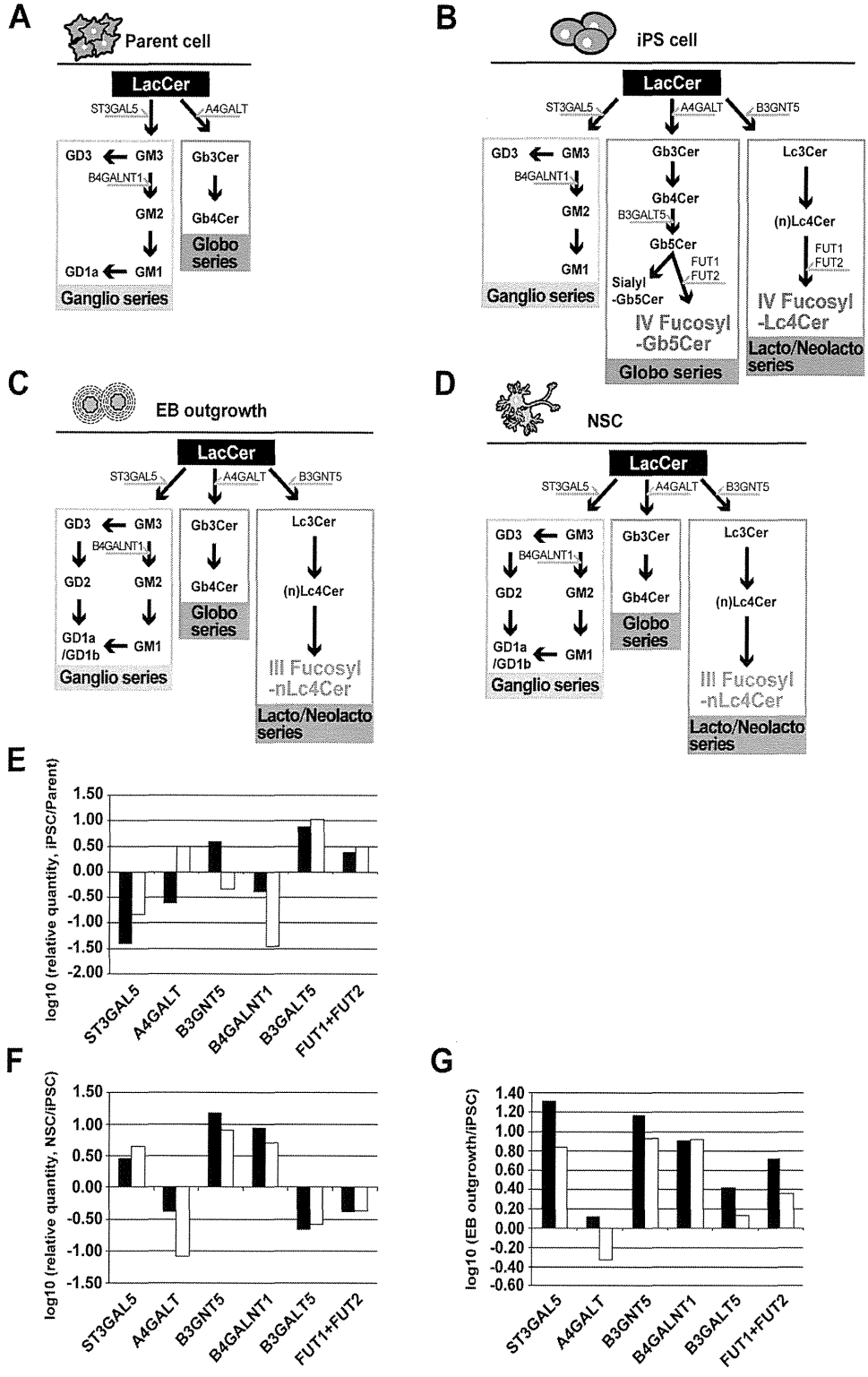

Figure 5. Biosynthetic pathways of GSLs and expression of glycosyltransferase genes. (**A**–**D**) Biosynthetic pathways of GSLs in parental cells (**A**), iPSCs (**B**), EB-outgrowth (**C**), and NSCs (**D**). (**E**) Relative quantity of glycosyltransferase genes expressed in MRC-iPSCs and UtE-iPSCs compared to their parental cells. The ratios of MRC-iPSC(#25)/MRC-5 (black columns) and UtE-iPSC(B05)/UtE (white columns) were plotted on a log scale bar graph. (**F**,**G**) Relative amount of glycosyltransferase genes expressed in iPSC-NSCs and iPSC-EB outgrowth against iPSCs. The ratios of iPSC-NSC/iPSCs (**F**) and iPSC-EB outgrowth/iPSCs (**G**) were plotted on a log scale bar graph. The black columns mean that the parental cells are MRC-5 cells, and the white columns mean that the parental cells are UtE cells. Akihiro Umezawa drew these figures by himself.

α1-2 fucosyltransferase (*FUT1/FUT2*). The expression of FUT1/FUT2 in hiPSCs showed a pronounced increase over their expression in the parental cells, and the biosynthesis of fucosyl Gb5Cer correlated with the up-regulation of FUT1/FUT2. The same genes also catalyze the biosynthesis of H type1 antigen. Indeed, IV fucosyl-(n)Lc4Cer in hiPSCs was detected by LC-MS, and the hiPSCs were positive for immunostaining with an anti-H type 1 antibody.

H antigen, the blood type O determinant, was detected in iPSCs. Although the parental cells, MRC5 and UtE5 cells, had genotypes of blood type O (OO) and type A (AO), respectively, both hiPSCs phenotypically expressed only H antigen. Cell surface ABO blood types are critical for transplantation of organs such as liver and kidney[24]. The expression of H antigen in hiPSCs, regardless of the parental genotype, has important ramifications for the use of hiPSCs in transplantation.

The GSLs in hESCs have been identified as globo- and lacto/neolacto-series GSLs including Gb4Cer, Gb5Cer, sialyl-Gb5Cer, fucosyl-Gb5Cer, Lc4Cer, and IV fucosyl-Lc4Cer, and using flow cytometry and mass spectrometry[16]. More recently, Barone et al. carried out the further identification of 18 kinds of globo- and lacto/neolacto-series GSLs including (n)Lc4Cer, H type1 pentaosylceramide and H type2 pentaosylceramide by mass spectrometry and proton NMR[18]. The GSLs observed in our study using hiPSCs have been also detected in hESCs. These results indicate that hiPSCs and hESCs display similar GSL synthetic pathways.

Recently, an antibody against SSEA-5 (H type 1 glycan) was proposed to detect hiPSCs and ESCs and remove teratoma-forming cells[25]. However, it has not been determined whether the carbohydrate antigen is glycolipid or glycoprotein in hiPSCs. More recently, an O-glycan comprising an H type 3 antigen structure in hiPSCs was identified using a high-throughput antibody-overlay lectin microarray[9]. These papers and our present study suggest that multiple structures of H antigen exist on the cell surface of hiPSCs.

Based on the GSL analysis for hiPSCs, fucosyl-Gb5Cer and IV fucosyl-(n)Lc5Cer appear to be good candidates as novel markers for validation and identification of hiPSCs. To determine the specificity of the two GSLs detected in undifferentiated hiPSCs, the GSLs in NSCs and EB outgrowth that were differentated from hiPSCs were also identified by LC-MS. Fucosyl-Gb5Cer and IV fucosyl-(n)Lc4Cer, as well as Gb5Cer and sialyl-Gb5Cer, were not detected in NSCs and EB outgrowth. The analysis of GSL-related glycosyltransferase genes suggest that the disappearance of Gb5Cer, sialyl-Gb5Cer, and fucosyl-Gb5Cer were caused by the increase of ST3GAL5 and B4GALNT5 activity, which are related to the biosynthesis of ganglio-series GSLs; and the decrease of A4GALT, which is related to the biosynthesis of globo-series GSLs.

The switching of the core structures of GSLs was observed for differentiation of hiPSCs as well as hESCs. Alteration of GSLs during differentiation of ESCs to EB outgrowth has also been reported[16]. It was also demonstrated that the core structures of GSLs in EB outgrowth switched from globo- and lacto/neolacto- to ganglio-series, and GM3 synthase (ST3GAL5) activity increased significantly. Furthermore, the switching of the core structures of GSLs from globo- and lacto/neolacto- to ganglio-series has been observed in mouse embryonic development as well as human ESC differentiation[5]. However, the expression of SSEA-1 in EB outgrowth, neural progenitor cells and definitive endoderm was not reported in this previous study. We found that SSEA-1 known as NSC marker was detected in NSCs and EB outgrowth by immunocytochemical analysis. The GSL structures corresponding to H type 1 antigen and SSEA-1 are isomers of fucosyl-(n)Lc4Cer. Though the sequences were determined by the MS/MS analyses, the isomers such as lacto- and neolacto-series could not be determined and the coexistence of the isomers could not be excluded by the MS/MS analyses. The proposed structures of the GSLs were deduced by the immunocytochemical analysis.

Interestingly, the cell type-specific major fatty acid length was detected: "C16:0 and C18:0" in iPSCs, and "C16:0 and C24:0" in parental cells, NSC, and EB cells. This difference in major fatty acid length may be attributed to the alteration in the biosynthesis of ceramide during the process of reprograming and differentiation.

In conclusion, we observed the GSL dynamics that occurs during reprogramming and differentiation of hiPSCs. The predominant GSL biosynthesis in undifferentiated hiPSCs consisted of globo- and lacto/neolacto-series GSLs including SSEA-3, SSEA-4, Globo H, and H type antigen, while those in parental somatic cells, NSC, and EB outgrowth were comprised of ganglio-series GSLs. Switching of GSLs from ganglio- to globo- and lacto/neolacto-series in hiPSCs may contribute to maintenance of the undifferentiated state and pluripotency. However, the roles of SSEA-3 (Gb5Cer), SSEA-4 (sialyl-Gb5Cer), Globo H (fusosyl-Gb5Cer), and H type1 antigen (IV fusosyl-Lc4Cer) in the functions of hiPSCs have not been clarified. It has been reported that SSEA-3 and Globo H were expressed in cancer stem cells[26], and that Globo H was expressed in breast cancer[27]. Therefore, analysis of the roles of globo- and lacto/neolacto-series GSLs in hiPSCs may help elucidate the mechanisms of generation and differentiation of cancer cells.

Methods

Cell Culture. hiPSCs were maintained with irradiated MEFs as previously described[8,22,23,28]. In this study, MRCiPS#16 (also called Fetch/NIHS0604 in other literature), MRCiPS#25 (Tic/JCRB1331), MRCiPS#40 (Skipper/NIHS0600), UtE-iPS-A07 (UtEiPS-07/QuarterBack), and UtE-iPS-B05 (UtEiPS-11/SplitEnd) were used for carbohydrate analysis. The MRC-iPSCs and UtE-iPSCs were generated from parental cells, MRC-5 cells and uterine endometrial cells (UtE, specimen number 1104). Differentiation of iPSCs into

NSC was carried out according to the standard protocol[29]. iPSCs were cultivated in medium for inducing differentiation into NSC for 7 days followed by NSC maintenance medium for 3 days (Supplemental Figure S2A, Supplemental Table S3A). Differentiation of iPSCs to EB outgrowth was carried out as follows: iPSCs were treated with 300PU/ml dispase II (Invitrogen) at 37 °C for 3 min. After removal of irrMEF (irradiated mouse embryonic fibroblast), colonies of iPSCs were collected by pipetting with EB medium (Supplemental Table S3B). The iPSCs were washed with EB medium three times. The cells were suspended with EB medium, and the cells were seeded onto Lipidure® Coat Dishes A-90 (NOF Co.), and incubated in 5% CO_2-95% air at 30 °C for 4 days. Thereafter, the cells were cultured in D-MEM/F-12 (Gibco) supplemented with 10% FBS (Gibco) and 1% penicillin/ streptomycin (Gibco) for 10 days. At 11days after the culture in D-MEM/F-12 (Gibco) supplemented with 10% FBS and 1% penicillin/ streptomycin, EB out growth was formed, and tridermic cells were observed.

Immunocytochemical analysis. Cells were fixed with 4% paraformaldehyde in PBS at 4 °C for 10 min. After washing with PBS, the cells were pre-hybridized with blocking buffer (10% goat serum in PBS) for 30 min at room temperature and then reacted with the primary antibodies in blocking buffer at 4 °C for 12 h. After washing with PBS, the cells were reacted with the secondary antibodies in blocking buffer for 30 min at room temperature. Primary and secondary antibodies are summarized in Supplemental Table S4A–C. The cells were counterstained with DAPI and mounted.

cDNA standards. Genes for A4GALT, ST3GAL5, B3GNT5, B4GALNT1, B3GALT5, FUT1, and FUT2 were amplified with primers shown in Supplemental Table S5A from cDNA prepared from MRC-5 cells (A4GALT and ST3GAL5), UtE cells (B4GALNT1), MRC5-iPSCs (B3GALT5), UtE-iPSCs (FUT1 and FUT2), and UET13 cells (B3GNT5) by PCR using KOD plus ver.2 (TOYOBO) or KOD plus neo (TOYOBO) and cloned into pENTR11 (Invitrogen) pGEM-T easy vector (Promega) and pcDNA3 (Invitrogen). cDNA plasmid concentrations were measured by optical density spectrometry and corresponding copy number was calculated using the following equation: 1 ng of 1000 bp DNA $= 9.1 \times 10^8$ molecules. Serial dilutions from the cDNA plasmid were used as standard curves, each containing a known amount of input copy number.

Quantitative RT-PCR. RNA was extracted from cells using the RNeasy Plus Mini kit (Qiagen). An aliquot of total RNA was reverse transcribed using an oligo(dT) primer. For the thermal cycle reactions, the cDNA template was amplified (ABI PRISM 7900HT Sequence Detection System) with primers shown in Supplemental Table S5B using the Platinum Quantitative PCR SuperMix-UDG with ROX (11743-100, Invitrogen) under the following reaction conditions: 40 cycles of PCR (95 °C for 15 s and 60 °C for 1 min) after an initial denaturation (95 °C for 2 min). Fluorescence was monitored during every PCR cycle at the annealing step. The authenticity and size of the PCR products were confirmed using a melting curve analysis (with software provided by Applied Biosystems) and gel electrophoresis analysis.

LC-MS/MS. Lipids were extracted from the cell pellets with chloroform/methanol (2:1, v/v) and chloroform/isopropanol/water (7:11:2, v/v) in a sonicating water bath. Total extracts were mixes and evaporated to dryness. Alkaline hydrolysis was performed to remove phospholipids. The lipid extracts without alkaline hydrolysis were also prepared. The lipids extracted from the cells were dissolved with chloroform/methanol (2:1, v/v) and 2 M KOH was added. After incubation at 37 °C for 3 hours, supernatants were collected and evaporated to dryness. The extracts were desalted using a SepPak C18 column (Waters) and analyzed by LC-MS. LC-MS employed in this study was electrospray ionization (ESI)/an ion trap mass spectrometer (HCT-Ultra 11S, Bruker Daltonics, Billerica, MA, USA) equipped with the ADVANCE UHPLC (AMR, Japan). The glycolipids were loaded onto a silica column (0.2 × 150 mm, Imtakt, Japan) equilibrated with solvent A (chloroform/methanol/water (C/M/W) containing 2 M ammonium acetate buffer, pH 5.5 (89/10/1, v/v/v)), and were eluted with a 0–100% linear gradient of solvent B (M/W containing 0.2 M ammonium acetate buffer, pH 5.5 (9/1, v/v)) in 60 min at a flow rate of 2000 nl/min. The ESI parameters were as follows: nebulizer, 7.0 psi; dry gas (N_2), 4.0 l/min; dry temperature, 300°C; capillary, −4 kV for negative ion mode. The mass recorded in survey acquisitions ranged from 150 through 1,800 m/z. NSC and hiPSCs were detected by multiple reaction monitoring mode for (iPSCs, NSCs, and EB outgrowth) and auto MS mode (parental cells).

ABO genotyping. Genomic DNA was isolated using the DNeasy kit (Qiagen) according to the manufacturer's protocol. ABO blood types were determined by the PCR-APLP method using the allele-specific primers[20]. In addition, exons 6 and 7 of the ABO transferase gene was sequenced after amplification by genomic PCR using specific primers[21].

Flow cytometry. Cells were stained for 1 h at 4 °C with primary antibodies and immunofluorescent secondary antibodies. The cells were then analyzed on a Cytomics FC 500 (Beckman Coulter, Inc.) and the data were analyzed with the FlowJo Ver. 7 (Tree Star, Inc.). Antibodies against human Globo H (ALX-804-550C050, Enzo Life Sciences, Inc.) and H antigen (anti-blood group H1 (O) antigen antibody:ab3355, abcam) were adopted as primary antibodies. Alexa Fluor 488 goat anti-mouse IgM (μ chain, A21042, Invitrogen) and Alexa Fluor 488 F(ab')2 fragment goat anti-mouse IgG (H + L) (A11017,

Invitrogen) were used as secondary antibodies when the primary antibodies were to Globo H and H antigen, respectively. Fluorescent-conjugated antibodies (555401, BD Pharmingen and FAB1435F, R&D) were used for the analyses of SSEA-1 and SSEA-4, respectively. Isotype antibodies were used as control (Supplemental Table S5C).

References

1. Takahashi, K. *et al.* Induction of pluripotent stem cells from adult human fibroblasts by defined factors. *Cell* **131,** 861–872 (2007).
2. Yu, J. *et al.* Induced pluripotent stem cell lines derived from human somatic cells. *Science* **318,** 1917–1920 (2007).
3. Hankowski, K. E., Hamazaki, T., Umezawa, A. & Terada, N. Induced pluripotent stem cells as a next-generation biomedical interface. *Lab Invest* **91,** 972–977 (2011).
4. Hakomori, S. Glycosylation defining cancer malignancy: new wine in an old bottle. *Proc Natl Acad Sci USA* **99,** 10231–10233 (2002).
5. Hakomori, S. I. Structure and function of glycosphingolipids and sphingolipids: recollections and future trends. *Biochim Biophys Acta* **1780,** 325–346 (2008).
6. Hakomori, S. I. Glycosynaptic microdomains controlling tumor cell phenotype through alteration of cell growth, adhesion, and motility. *FEBS Lett* **584,** 1901–1906 (2010).
7. Nishijima, Y. *et al.* Glycan profiling of endometrial cancers using lectin microarray. *Genes Cells* **17,** 826–836 (2012).
8. Toyoda, M. *et al.* Lectin microarray analysis of pluripotent and multipotent stem cells. *Genes Cells* **16,** 1–11 (2011).
9. Tateno, H. *et al.* Podocalyxin is a glycoprotein ligand of the human pluripotent stem cell-specific probe rBC2LCN. *Stem Cells Transl Med* **2,** 265–273 (2013).
10. Wang, Y. *et al.* Glycosylation of Nalpha-lauryl-O-(beta-D-xylopyranosyl)-L-serinamide as a saccharide primer in cells. *Carbohydr Res* **361,** 33–40 (2012).
11. Sato, T., Hatanaka, K., Hashimoto, H. & Yamagata, T. Syntheses of oligosaccharides using cell function. *Trends in Glycoscience and Glycotechnology* **19,** 1–17 (2007).
12. Kaneko, T. *et al.* Neuroblastoma cells can be classified according to glycosphingolipid expression profiles identified by liquid chromatography-tandem mass spectrometry. *Int J Oncol* **37,** 1279–1288 (2010).
13. Ogasawara, N. *et al.* Accelerated biosynthesis of neolacto-series glycosphingolipids in differentiated mouse embryonal carcinoma F9 cells detected by using dodecyl N-acetylglucosaminide as a saccharide primer. *J Biochem* **149,** 321–330 (2011).
14. Zhu, X., Hatanaka, K., Yamagata, T. & Sato, T. Structural analysis of glycosphingolipid analogues obtained by the saccharide primer method using CE-ESI-MS. *Electrophoresis* **30,** 3519–3526 (2009).
15. Fujitani, N. *et al.* Total cellular glycomics allows characterizing cells and streamlining the discovery process for cellular biomarkers. *Proc Natl Acad Sci USA* **110,** 2105–2110 (2013).
16. Liang, Y. J. *et al.* Switching of the core structures of glycosphingolipids from globo- and lacto- to ganglio-series upon human embryonic stem cell differentiation. *Proc Natl Acad Sci USA* **107,** 22564–22569 (2010).
17. Liang, Y. J. *et al.* Changes in glycosphingolipid composition during differentiation of human embryonic stem cells to ectodermal or endodermal lineages. *Stem Cells* **29,** 1995–2004 (2011).
18. Barone, A. *et al.* Structural complexity of non-acid glycosphingolipids in human embryonic stem cells grown under feeder-free conditions. *J Biol Chem* **288,** 10035–10050 (2013).
19. Kannagi, R. *et al.* Stage-specific embryonic antigens (SSEA-3 and -4) are epitopes of a unique globo-series ganglioside isolated from human teratocarcinoma cells. *Embo j* **2,** 2355–2361 (1983).
20. Muro, T. *et al.* Determination of ABO genotypes by real-time PCR using allele-specific primers. *Leg Med (Tokyo)* **14,** 47–50 (2012).
21. Ota, M., Fukushima, H., Kulski, J. K. & Inoko, H. Single nucleotide polymorphism detection by polymerase chain reaction-restriction fragment length polymorphism. *Nat Protoc* **2,** 2857–2864 (2007).
22. Nishino, K. *et al.* DNA Methylation Dynamics in Human Induced Pluripotent Stem Cells over Time. *PLoS Genet* **7,** e1002085 (2011).
23. Nishino, K. *et al.* Defining hypo-methylated regions of stem cell-specific promoters in human iPS cells derived from extra-embryonic amnions and lung fibroblasts. *PLoS One* **5,** e13017 (2010).
24. Mölne, J. *et al.* Blood group ABO antigen expression in human embryonic stem cells and in differentiated hepatocyte- and cardiomyocyte-like cells. *Transplantation* **86,** 1407–1413 (2008).
25. Tang, C. *et al.* An antibody against SSEA-5 glycan on human pluripotent stem cells enables removal of teratoma-forming cells. *Nat Biotechnol* **29,** 829–834 (2011).
26. Chang, W. W. *et al.* Expression of Globo H and SSEA3 in breast cancer stem cells and the involvement of fucosyl transferases 1 and 2 in Globo H synthesis. *Proc Natl Acad Sci USA* **105,** 11667–11672 (2008).
27. Wang, C. C. *et al.* Glycan microarray of Globo H and related structures for quantitative analysis of breast cancer. *Proc Natl Acad Sci USA* **105,** 11661–11666 (2008).
28. Makino, H. *et al.* Mesenchymal to embryonic incomplete transition of human cells by chimeric OCT4/3 (POU5F1) with physiological co-activator EWS. *Exp Cell Res* **315,** 2727–2740 (2009).
29. Chambers, S. M. *et al.* Highly efficient neural conversion of human ES and iPS cells by dual inhibition of SMAD signaling. *Nat Biotechnol* **27,** 275–280 (2009).

Acknowledgments

We would like to express our sincere thanks to K. Iijima for providing expert technical assistance, K. Minami for the support throughout the work, Dr. C. Ketcham for English editing and proofreading, and E. Suzuki, Y. Suehiro, and K. Saito for secretarial work. This research was supported by grants from the Ministry of Education, Culture, Sports, Science, and Technology (MEXT) of Japan; by Ministry of Health, Labour and Welfare Sciences (MHLW) research grants; by a Research Grant on Health Science focusing on Drug Innovation from the Japan Health Science Foundation; by the program for the promotion of Fundamental Studies in Health Science of the Pharmaceuticals and Medical Devices Agency; by the Grant of National Center for Child Health and Development; by Research Seeds Quest Program from the Japan Science and Technology Agency (JST). We acknowledge the International High Cited Research Group (IHCRG #14-104), Deanship of Scientific Research, King Saudi University, Riyadh, Kingdom of Saudi Arabia. AU thanks King Saud University, Riyadh, Kingdom of Saudi Arabia, for the Visiting Professorship.

Author Contributions

T.S. and A.U. designed experiments.T.O., E.S., S.S., M.T., H.N. and M.Y.I. performed experiments. T.O., E.S., M.T., T.S. and A.U. analyzed data. Y.M., N.K. and J.F. contributed reagents, materials and analysis tools. T.S. and A.U. wrote this manuscript.

Additional Information

Supplementary information accompanies this paper at http://www.nature.com/srep

Competing financial interests: The authors declare no competing financial interests.

How to cite this article: Ojima, T. *et al.* Glycolipid dynamics in generation and differentiation of induced pluripotent stem cells. *Sci. Rep.* **5**, 14988; doi: 10.1038/srep14988 (2015).

ELSEVIER

CrossMark

Experimental Hematology

Experimental Hematology 2016;44:68–74

BRIEF COMMUNICATIONS

GSK3β inhibition activates the *CDX/HOX* pathway and promotes hemogenic endothelial progenitor differentiation from human pluripotent stem cells

Kenji Kitajima[a], Marino Nakajima[a,b], Mai Kanokoda[a,b], Michael Kyba[c], Abhijit Dandapat[c], Jakub Tolar[d], Megumu K. Saito[e], Masashi Toyoda[f], Akihiro Umezawa[g], and Takahiko Hara[a,b]

[a]*Stem Cell Project, Tokyo Metropolitan Institute of Medical Science, Tokyo, Japan;* [b]*Graduate School of Medical and Dental Sciences, Tokyo Medical and Dental University, Tokyo, Japan;* [c]*Lillehei Heart Institute, Department of Pediatrics, University of Minnesota, Minneapolis, MN;* [d]*Pediatric Hematology–Oncology, Blood and Marrow Transplantation, University of Minnesota, Minneapolis, MN;* [e]*Clinical Application Department, Center for iPS Cell Research and Application, Kyoto University, Kyoto, Japan;* [f]*Research Team for Geriatric Medicine (Vascular Medicine), Tokyo Metropolitan Institute of Gerontology, Tokyo, Japan;* [g]*Department of Reproductive Biology and Pathology, National Research Institute for Child Health and Development, Tokyo, Japan*

(Received 27 May 2015; revised 25 September 2015; accepted 27 September 2015)

WNT/β-CATENIN signaling promotes the hematopoietic/endothelial differentiation of human embryonic stem cells and human induced pluripotent stem cells (hiPSCs). The transient addition of a GSK3β inhibitor (GSKi) has been found to facilitate in vitro endothelial cell differentiation from hESCs/hiPSCs. Because hematopoietic and endothelial cells are derived from common progenitors (hemogenic endothelial progenitors [HEPs]), we examined the effect of transient GSKi treatment on hematopoietic cell differentiation from hiPSCs. We found that transient GSKi treatment at the start of hiPSC differentiation induction altered the gene expression profile of the cells. Multiple *CDX/HOX* genes, which are expressed in the posterior mesoderm of developing embryos, were significantly upregulated by GSKi treatment. Further, inclusion of the GSKi in a serum- and stroma-free culture with chemically defined medium efficiently induced HEPs, and the HEPs gave rise to various lineages of hematopoietic and endothelial cells. Therefore, transient WNT/β-CATENIN signaling triggers activation of the *CDX/HOX* pathway, which in turn confers hemogenic posterior mesoderm identity to differentiating hiPSCs. These data enhance our understanding of human embryonic hematopoietic/endothelial cell development and provide a novel in vitro system for inducing the differentiation of hematopoietic cells from hiPSCs.

Human induced pluripotent stem cells (hiPSCs) are a promising source of cells for regenerative medicine, drug screening, and pathogenetic studies of incurable diseases [1]. In addition, hematopoietic cells derived from hiPSCs may be used for transfusion and immunotherapy. To support these applications, an efficient and reliable in vitro differentiation induction system for producing hematopoietic cells from hiPSCs is needed.

Offprint requests to: Kenji Kitajima, Stem Cell Project, Tokyo Metropolitan Institute of Medical Science, 2-1-6 Kamikitazawa, Setagaya-ku, Tokyo 156-8506, Japan; E-mail: kitajima-kj@igakuken.or.jp

Supplementary data related to this article can be found online at http://dx.doi.org/10.1016/j.exphem.2015.09.007.

WNT/β-CATENIN signaling promotes the hematopoietic differentiation of human embryonic stem cells (hESCs) [2]. Recent reports have indicated that endothelial differentiation from hESCs/hiPSCs is enhanced by transient treatment with a GSK3β inhibitor (GSKi) [3,4]. However, the roles of WNT/β-CATENIN signaling in hematopoietic/endothelial cell differentiation from hESCs/hiPSCs remain to be clarified. During gastrulation, epiblasts ingress through the primitive streak (PS) and give rise to mesoderm cells via the epithelial-to-mesenchymal transition (EMT) [5,6]. PS formation and EMT induction are severely impaired in mouse embryos lacking the Wnt/β-catenin pathway [5,6]. Therefore, we hypothesized that WNT/β-CATENIN signaling enhances the hematopoietic/

0301-472X/
http://dx.doi.org/10.1016/j.exphem.2015.09.007

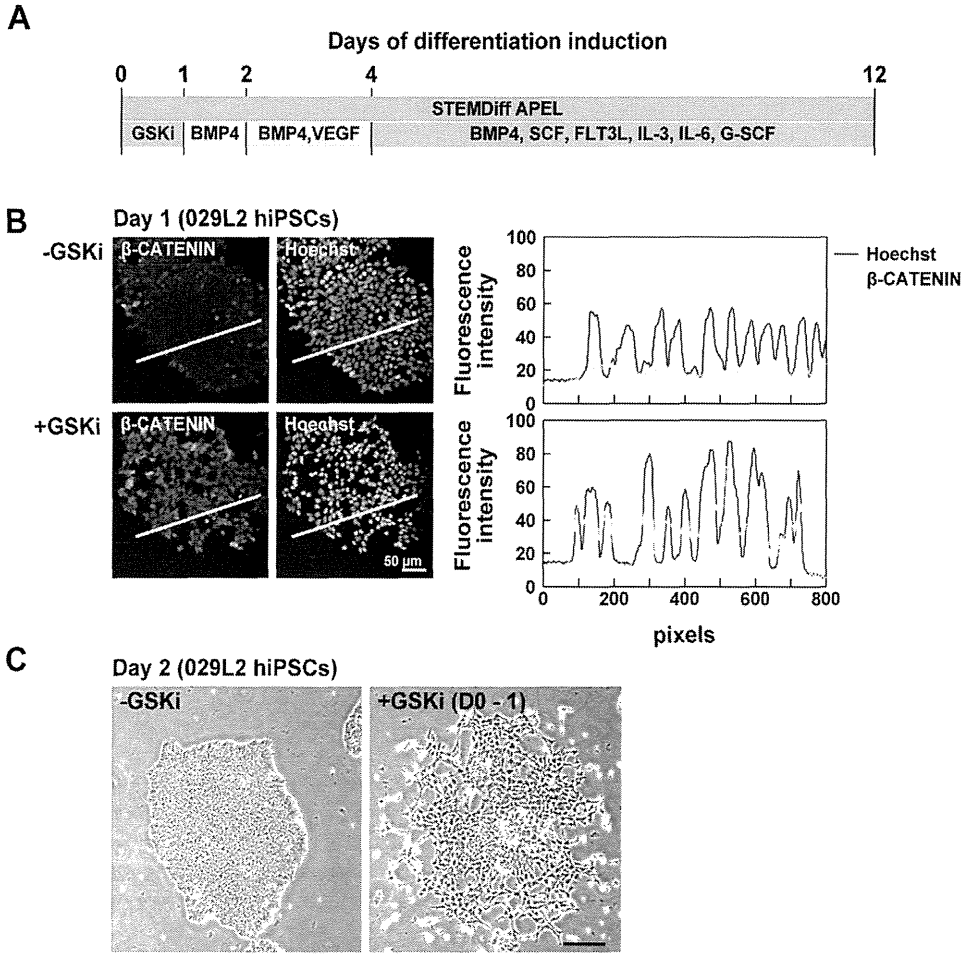

Figure 1. Effects of GSKi treatment on EMT of hiPSCs. (**A**) Schematic diagram of in vitro differentiation protocol of hiPSCs. Human induced progenitor stem cells were cultured in STEMDiff APEL with or without GSKi (days 0–1). GSKi was then removed, and BMP4 (days 1–4) and VEGF (days 2–4) were added. On days 4 and 8, medium was changed to STEMDiff APEL containing BMP4, SCF, FLT3L, IL-6, IL-3, and G-CSF. (**B**) Nuclear accumulation of β-CATENIN by GSKi. The 029L2 hiPSCs were differentiated in STEMDiff APEL with or without GSKi for 1 day. Left: Microscopic images. Right: Relative fluorescence intensities of β-CATENIN signals and Hoechst stains (*white lines* in left panels) were quantified. (**C**) Morphology of 029L2 hiPSC colonies treated with or without GSKi (days 0–1) followed by 1 day of culture with BMP4. Bar = 200 μm.

endothelial differentiation of hESCs/hiPSCs by facilitating PS formation and EMT induction.

Here, we demonstrate that the transient addition of CHIR99021, a GSKi, greatly improved the differentiation of hiPSCs into hemogenic endothelial progenitors (HEPs) and hematopoietic cells. GSKi treatment also resulted in the upregulation of *CDX/HOX* genes, suggesting that WNT/β-CATENIN signaling triggers activation of the *CDX/HOX* pathway, which promotes hematopoietic/endothelial cell differentiation from hiPSCs.

Methods

The hiPSC lines are listed in Supplementary Table E1 (online only, available at www.exphem.org). The in vitro differentiation protocol for hiPSCs has been described [3] with some modifications (Fig. 1A). First, single-cell suspensions of hiPSCs (10^4 to 10^5) were placed onto 60-mm culture dishes coated with growth factor-reduced Matrigel (BD Biosciences, San Jose, CA) in mTeSR1 (STEMCELL Technologies, Vancouver, BC, Canada) with 10 μmol/L rock inhibitor (rocki) (Y-27632, WAKO, Tokyo) (day −4). Two days later, medium was replaced by mTeSR1 without rocki. On day 0, the cells were washed twice with phosphate-buffered saline (PBS) and cultured in STEMDiff APEL medium (STEMCELL Technologies) with or without 5 μmol/L GSKi (CHIR99021, WAKO). On day 1, the cells were washed twice with PBS and cultured in STEMDiff APEL medium with 25 ng/mL human bone morphogenic protein 4 (BMP4, R&D Systems, Minneapolis, MN). The next day, 40 ng/mL human vascular endothelial growth factor 165 (VEGF, R&D Systems) was added. The effects of WNT inhibition were analyzed by addition of 150 ng/mL Dickkopf-related protein 1 (Dkk1, Peprotech, Rocky Hill, NJ). On days 4 and 8, medium was replaced by STEMDiff APEL containing 300 ng/mL human stem cell factor (SCF, R&D systems), 300 ng/mL human Fms-related tyrosine kinase ligand (FLT3L, R&D Systems), 10 ng/mL human interleukin-6 (IL-6, Peprotech), 10 ng/mL human interleukin-3 (IL-3, Peprotech), 50 ng/mL human granulocyte colony-stimulating factor (G-CSF, Peprotech), and 25 ng/mL human BMP4. Use of this cytokine combination was originally described by Chadwick et al. [7].

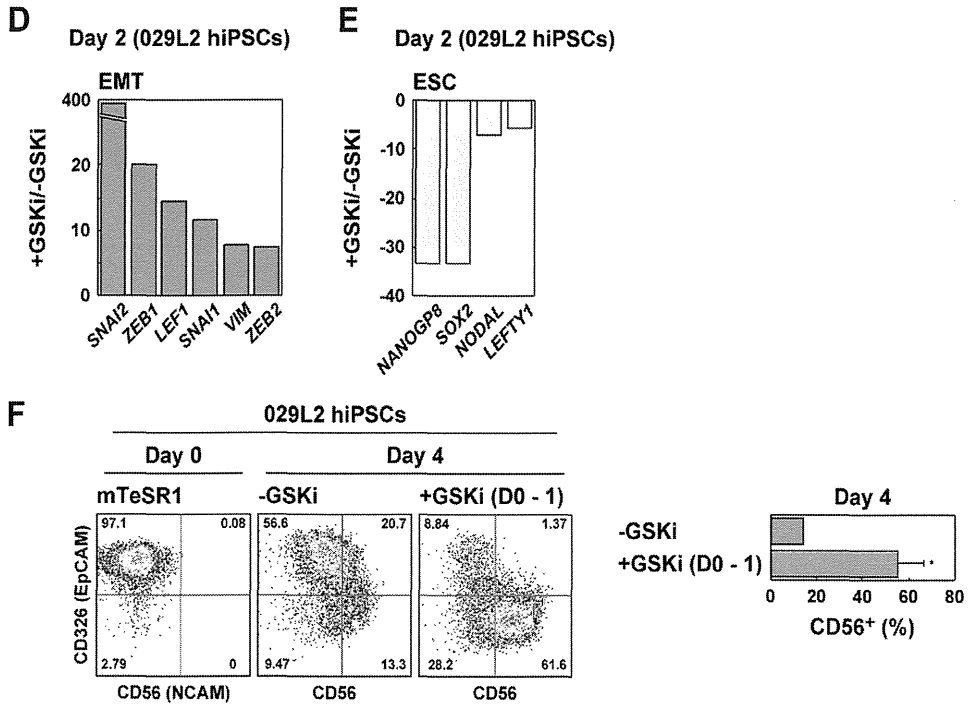

Figure 1. (*continued*) (**D**) EMT-related upregulated genes in the GSKi-treated hiPSCs. On day 2, RNA was collected from the differentiated 029L2 hiPSCs treated with GSKi (days 0–1) or without GSKi and subjected to microarray analysis. (**E**) ESC marker genes downregulated in the GSKi-treated 029L2 hiPSCs. (**D, E**) Fold changes in relative expression level (+GSKi/−GSKi). (**F**) The 029L2 hiPSCs were differentiated in STEMDiff APEL with or without GSKi (days 0–1), followed by 3 days of culture with BMP4 and VEGF, as illustrated in (**A**). On day 4, expression of CD326 and CD56 was analyzed by FACS. Average percentages of $CD56^+$ cells ($n = 4$) ± SD are on the right ($^*p < 0.005$).

The differentiated cells were harvested by Accumax cell dissociation reagent (Innovative Cell Technologies, San Diego, CA) and analyzed by FACSAriaIII (BD Biosciences) and LSRFortessa X-21 (BD Biosciences). The cells were also analyzed by culturing in MethoCult H4034 (STEMCELL Technologies). OP9 cells were used as described previously [8]. The cytokines and antibodies used are listed in Supplementary Tables E2–E4 (online only, available at www.exphem.org). A microarray analysis was carried out using 3-D Gene Human Oligo Chip 24k (Toray, Tokyo, Japan). Detailed methods are provided in the Supplementary Methods (online only, available at www.exphem.org).

Results and discussion

Upregulation of EMT-related genes and CDX/HOX genes by early GSKi treatment

First, we confirmed the nuclear accumulation of β-CATENIN in GSKi-treated hiPSCs (029L2) (Fig. 1B). Next, the GSKi was removed on day 1 of differentiation induction, and BMP4 was added for mesoderm induction (Fig. 1A). We noticed morphologic changes in the hiPSC colonies on day 2. At this point, the GSKi-treated hiPSC colonies became loose, and the cells at the periphery of each colony were scattered, whereas the cells in the untreated hiPSC colonies remained tightly packed (Fig. 1C).

To examine the gene expression profile of differentiated hiPSCs after early GSKi treatment, we performed a microarray analysis on day 2 of differentiation induction. Compared with the untreated cells, 217 genes, including EMT-related genes [9], were significantly upregulated (more than fivefold) in GSKi-treated cells (Fig. 1D; Supplementary Table E5, online only, available at www.exphem.org). On the other hand, 148 genes, including ESC markers [10], were significantly downregulated (less than fivefold) by GSKi treatment (Fig. 1E, Supplementary Table E6, online only, available at www.exphem.org). The induction of EMT by GSKi treatment was confirmed based on downregulation of CD326 (EpCAM) and induction of CD56 (NCAM) (Fig. 1F).

Strikingly, all *CDX* genes (*CDX1*, *2*, and *4*) and six *HOX* genes were strongly upregulated by GSKi treatment (Fig. 2A). Because *Cdx* genes are expressed in the posterior mesoderm [11], early GSKi treatment appeared to induce posterior mesoderm cells from hiPSCs. Anterior *HOX* genes (*HOXB2* and *HOXA1*), cardiac lineage-related genes (*TBX3, HAND1*, and *NKX2-5*), and multiple mesoderm/mesendoderm markers were also upregulated by early GSKi treatment, whereas axial mesoderm markers such as *GSC*, *CER1*, *CHRD*, and *FOXA2* [12] were unaffected (Fig. 2B). Given the finding that GSKi treatment induces robust cardiac differentiation of hESCs [13], early GSKi treatment induced not only posterior mesoderm cells, but also anterior/cardiac mesoderm cells.

The Wnt effector *Lef1* has been found to regulate *Cdx* gene expression [14–16]. According to our data, four *WNT* family genes and *LEF1* were significantly upregulated